frontiers | Frontiers in Earth Science

TYPE Original Research
PUBLISHED 19 May 2025
DOI 10.3389/feart.2025.1499533

OPEN ACCESS

EDITED BY
Ahmed E. Radwan,
Jagiellonian University, Poland

REVIEWED BY
Shuai Yin,
Xi'an Shiyou University, China
Xu Shenglin,
Chengdu University of Technology, China

*CORRESPONDENCE
Lixue Cheng,
415066437@qq.com

RECEIVED 21 September 2024
ACCEPTED 19 March 2025
PUBLISHED 19 May 2025

CITATION
Cheng L and Peng J (2025) Controls on lacustrine shale reservoir characteristics: insights from deposition, diagenesis, and geochemistry in the Jurassic Qianfoya Formation.
Front. Earth Sci. 13:1499533.
doi: 10.3389/feart.2025.1499533

Controls on lacustrine shale reservoir characteristics: insights from deposition, diagenesis, and geochemistry in the Jurassic Qianfoya Formation

Lixue Cheng[1,2]* and Jun Peng[1]

[1]School of Geoscience and Technology, Southwest Petroleum University, Chengdu, China, [2]College of Air Traffic Management, Civil Aviation Flight University of China, Guanghan, China

Continental lacustrine shales, which are distinct from marine shales in reservoir architecture, pose challenges for resource evaluation due to their complex multi-scale controls. The Middle Jurassic Qianfoya Formation in the Langzhong–Yuanba (LZ-YB) area of the northeastern Sichuan Basin represents a critical continental shale gas target, yet systematic studies of its reservoir quality drivers remain limited. Through integrated sedimentological, geochemical, and petrophysical analyses of core samples, three dominant sedimentary facies are identified: blocky, banded, and laminated, reflecting depositional energy variations. The formation shows favorable hydrocarbon potential with an average total organic carbon (TOC) content of 1.85% and is mineralogically dominated by clay minerals (illite and illite–smectite) and felsic components. Semi-deep lacustrine facies, especially clay-rich lithofacies, demonstrate superior reservoir quality due to higher total organic carbon content and pore networks dominated by silty intergranular pores, interlayer pores in clay minerals, and intragranular pores in pyrite and microfractures, contrasting with marine shales where organic matter-hosted pores prevail. Key controlling factors include organic matter-clay mineral synergy, depositional environment (anoxic conditions, freshwater influx, and terrigenous input), and diagenetic processes such as clay transformation and recompaction. Laminated facies exhibit optimal reservoir quality compared to blocky or banded types, with positive correlations between clay-organic content and storage capacity. These findings highlight the coupled depositional–diagenetic controls on continental shale reservoirs, providing critical insights for global exploration of analogous lacustrine shale systems.

KEYWORDS

lacustrine shale, reservoir characteristics, depositional–diagenetic controls, organic-clay synergy, Qianfoya formation, continental shale reservoirs

1 Introduction

Global advancements in unconventional resource exploration have revealed substantial potential in continental shale systems beyond traditional marine targets. Successful cases include the lacustrine Wolfcamp Formation in the Permian Basin (United States)

with estimated recoverable resources exceeding 20 billion barrels, the organic-rich Cretaceous La Luna Shale in South America, and the Permian Whitehill Formation in the Karoo Basin (South Africa), with total organic carbon (TOC) values as high as 14% (Iacoviello et al., 2019; Milkov et al., 2020; Sohail et al., 2022; Hakimi et al., 2023; Li et al., 2023). In China, recent discoveries highlight prolific continental shale plays, such as the Qingshankou Formation (Songliao Basin), the Chang 7 Member (Ordos Basin), and the Qianfoya (QFY) Formation (Sichuan Basin), which collectively hold over 10 billion tons of shale oil resources (Fan et al., 2020; Jin et al., 2022; Wang and Tang, 2023; Ma and Feng, 2023; Wang E. Z et al., 2023; Bian, 2024; Li H. et al., 2024; Li et al., 2024 J.; Li H et al., 2025). The marine shale of the Lower Silurian Longmaxi Formation in Southern Sichuan is the most typical shale gas reservoir in our country (Li, 2022; Li, 2023a; Radwan et al., 2023; He et al., 2025), while the continental shale strata of the Middle Jurassic QFY Formation is an important alternative area for exploration and development of shale oil and gas in the Sichuan Basin (Li et al., 2023c; Wu et al., 2024). In recent years, the Sinopec Group has successively deployed many exploration wells for the QFY Formation in the Langzhong-Yuanba (LZ-YB) area, northeastern Sichuan Basin, and better oil and gas shows have appeared. However, no commercial breakthrough has been achieved (Zhao et al., 2021; Zhang et al., 2021; Guo et al., 2022).

In the previous research on continental fine-grained sedimentary rocks, in the early stage, scholars around the world mostly studied the single and two controlling factors of reservoir quality (Jadoon et al., 2016; He et al., 2021; He et al., 2022; Liu J et al., 2024; Kasala et al., 2025; Ye et al., 2025; Hou et al., 2025). For example, Dai et al. believed that the total organic carbon (TOC) content and brittle mineral content in the continental shale reservoir of the Yanchang Formation in Ordos are the main factors controlling the development of nanoscale pores (Dai et al., 2016). According to the relationship between diagenetic sequence and pore evolution of the Paleogene lacustrine shale oil reservoir in the Dongying Depression, Zhang et al. suggested that the dissolution and hydrocarbon generation of organic matter can increase reservoir physical properties (Zhang et al., 2018). When Jadoon studied the lacustrine sedimentary environment of Roseneath and Murteree in Australia, it was found that organic-rich shale mainly developed in semi-deep and deep lake environments near the storm wave base (Jadoon et al., 2016). Natural fractures in shale oil formations play a significant role in fluid flow channels. Dong et al. proposed a fracture identification method (FRNN) based on deep learning, and the research results have been applied to the shale of the Yanchang Formation (Dong et al., 2024).

There is still no detailed study on the controlling factors of lacustrine fine-grained sedimentary reservoirs of the Middle Jurassic QFY Formation in the northeastern Sichuan Basin. Therefore, this paper systematically studies the main controlling factors affecting the reservoir quality of fine-grained sedimentary rocks in the QFY Formation from many aspects, which is significant for exploring the mechanism of petroleum enrichment in continental fine-grained sedimentary rocks and promoting the exploration of Jurassic continental shale gas in the northern Sichuan Basin.

2 Geological setting

The area under investigation is situated at the intersection of the depression in the northern Sichuan Basin and the low structural belt in the middle Sichuan Basin, crossing the Zitong–Cangxi nose structural belt, the NE structural belt, the depression in the northern Sichuan Basin, and the Yilong–Pyeongchang low structural belt, bordering the northern front of the Longmenshan in the west, the Micangshan uplift in the north, and the Dabashan arc structural belt in the east (Li et al., 2019; Sun, 2023; Qin and Lan, 2024; Hu et al., 2025) (Figure 1A). Since the Indo-China Movement, the orogenic belts in the margin of the basin (Longmenshan in the northwest and Micangshan in the north) began to uplift successively , providing many sedimentary materials for the study area. Because it is located inside the basin and far from the orogenic belt in the margin of the basin, the tectonic compression is not intensive in the study area, and the overall structure is simple, locally forming low-amplitude fold deformation and developing small-scale faults.

The Middle–Lower Jurassic strata in the LZ-YB area are developed and widely distributed. Controlled by tectonic subsidence of the basin with different orders and lake transgressions, organic-rich shales of semi-deep lacustrine subfacies are developed in the QFY Formation. As there are good terrestrial source rocks and shale reservoirs in the region, it has a huge oil and gas resource potential. According to the lithology, electrical properties, and oil and gas content, the QFY Formation can be divided vertically into 1st Member, 2nd Member, and 3rd Member from bottom to top, and it experiences an entire cycle of lake transgression-regression (Qiu et al., 2021) (Figure 1B). The lake transgressions continue from the 1st Member of the QFY Formation and reach the maximum flooding period in the 2nd Member. The black shale, dominated by semi-deep lacustrine subfacies, is developed, with a small amount of siltstone and fine sandstone. The shale is rich in organic matter and is of good quality (Chen, 2022). From then on, the lake regression gradually begins until the 3rd Member of the QFY Formation. The study area is a sedimentary system of shallow lake-semi-deep lake subfacies and develops sedimentary micro-facies, such as shallow lacustrine facies mudstone, semi-deep lacustrine facies mudstone, and various beach bars. The depth of the sedimentary water gradually increases from north to south.

3 Samples and methods

3.1 Samples

A multifaceted approach was adopted to investigate the reservoir characteristics and controlling factors influencing the quality of continental fine-grained sedimentary rocks within the Middle Jurassic QFY Formation in the LZ-YB area, northeastern Sichuan Basin. A total of 87 core samples were carefully collected from different lithofacies identified in several exploration wells, encompassing claystones, silty claystones, silt-bearing claystones, siltstones, muddy siltstones, and shell limestone. Before analysis, all core samples were cleaned, dried, and cut into smaller representative subsamples.

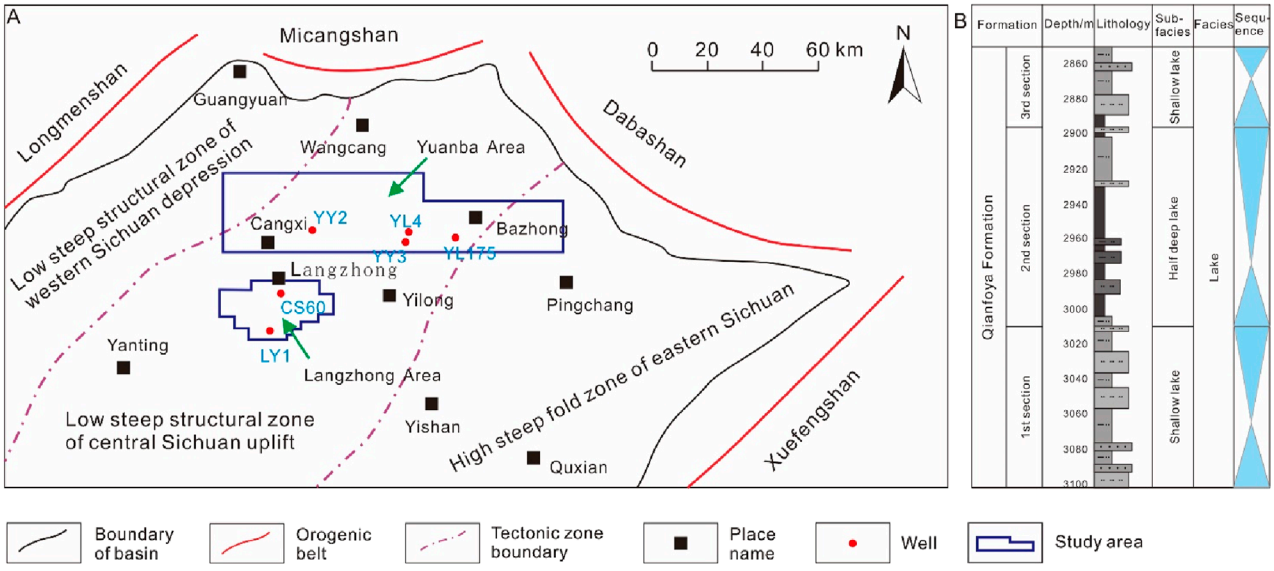

FIGURE 1
Geological setting of the LZ-YB area in the northeastern Sichuan Basin. **(A)** Structural location. **(B)** Stratigraphic column diagram.

3.2 Methods

Detailed macroscopic core observations were performed using a binocular microscope to document rock structures, including bedding characteristics (e.g., massive, banded, and laminated), bioturbation features, and any other visible rock structures indicative of the depositional environment. The lithological variations were documented by observing grain size variations, mineral composition based on visual inspection, and color changes. Additionally, any visible fractures were characterized based on their presence, orientation, and characteristics (e.g., open, filled, and mineralized), and evidence of hydrocarbons, such as oil staining, fluorescence, or gas shows, were recorded.

3.2.1 TOC analysis

The hydrocarbon generation potential of the QFY Formation was assessed by analyzing the TOC content of selected shale samples using a LECO CS-230 carbon-sulfur analyzer (He et al., 2022). Powdered samples were treated with hydrochloric acid (HCl) to remove carbonate minerals, and the TOC content was determined by combusting the treated samples at high temperatures in an oxygen-rich environment and measuring the evolved carbon dioxide (CO_2) using an infrared detector.

3.2.2 Whole-rock mineral composition analysis

The mineralogical composition of the core samples was determined through whole-rock X-ray diffraction (XRD) analysis. Representative rock samples were ground to a fine powder using a mortar and pestle and analyzed using a Bruker D8 Advance X-ray diffractometer. The resulting diffraction patterns were analyzed to identify and quantify the relative abundance of mineral phases, including quartz, clay minerals (e.g., illite, smectite, kaolinite, and chlorite), carbonate minerals (e.g., calcite and dolomite), and feldspar (Yang L. R et al., 2022; Nag et al., 2025; Peng et al., 2025). In whole-rock XRD analysis of fine-grained continental sedimentary rocks, acid combinations must be selected for sample digestion according to the mineral composition and target elements. HF + HNO_3 was used in this study, and the digestion process was as follows: (1) Sample preparation: ground to less than 200 mesh to ensure uniformity. (2) Acid mixing: 0.1–0.5 g of the sample was weighed into a polytetrafluoroethylene (PTFE) digestion tank, and 5–10 mL of HNO_3 and 3–5 mL of HF were added. (3) Closed digestion: using a microwave digester or high-pressure digester, the sample was heated to 180°C–200°C for 2–4 h (4) Acid treatment: After digestion, the solution was dried, and HNO_3 was added to redissolve and dry again (to remove residual HF and prevent damage to the ICP-MS atomizer). (5) Volume: Diluted HNO_3 (2%–5%) was added to bring the volume to 25–50 mL. The solution was filtered and tested on the machine.

3.2.3 Physical property analysis

Porosity and permeability, key parameters for reservoir quality assessment, were measured on cylindrical core plugs extracted from representative samples. Porosity was measured using a helium porosimeter (e.g., Quantachrome UltraPore) which measures the volume of helium gas permeating into the pore spaces of a core plug at a known pressure (Peng et al., 2018). Permeability, a measure of the ability of the rock to transmit fluids, was measured using a nitrogen gas permeameter (e.g., Vinci Technologies Permeameter) by flowing nitrogen gas through the core plug at a controlled pressure gradient and measuring the flow rate and pressure drop (Wen et al., 2024).

3.2.4 Reservoir pore characteristics

Scanning electron microscopy (SEM) was employed to visualize the pore structure and morphology of the QFY Formation. Small rock chips were mounted on SEM stubs, coated with gold to

prevent charging during imaging, and imaged using a high-resolution scanning electron microscope (e.g., FEI Quanta). Argon ion polishing was used to remove surface irregularities and expose the internal pore structure for better visualization. Large area backscattering scanning electron microscopy (MAPS) imaging technology, a technique that involves acquiring and stitching multiple high-resolution SEM images, was used to create a mosaic image of the sample surface (Jun and Liang, 2024). This approach allowed for the identification and quantification of different pore types (intergranular pores, interlayer pores in clay minerals, organic matter-hosted pores, and microfractures) based on their size, shape, and connectivity.

3.2.5 Geochemical analysis

Geochemical analyses were performed to determine the concentrations of specific elements and to understand the paleoenvironmental conditions during the deposition of the QFY Formation. Rock samples were digested using a combination of acids, and the concentrations of V, Cr, Ni, Sr, Ba, Al, Fe, Mn, and Mg were measured using inductively coupled plasma mass spectrometry (ICP-MS) or inductively coupled plasma atomic emission spectrometry (ICP-AES). The measured elemental concentrations were used to calculate various paleoenvironmental proxies, including V/Cr and V/(V + Ni) ratios for redox conditions, Sr/Ba ratios for paleosalinity, total rare earth elements (∑REE) and Fe/Mn and Mg/Ca ratios for paleoclimate, and Al content for paleoproductivity (Tang et al., 2023).

Diagenetic analysis was performed to evaluate the impact of post-depositional processes on the reservoir quality of the QFY Formation. Thin sections of selected core samples were prepared and examined under a polarized light microscope to identify diagenetic features, including compaction, cementation, dissolution, and clay mineral transformations. The compaction ratio was estimated based on the intensity of diagenetic alterations observed in the thin sections. The porosity loss due to cementation was evaluated using the Houseknecht method , which involves comparing the measured porosity with a theoretically calculated porosity based on the initial mineralogy of the rock.

4 Results

4.1 Reservoir petrological characteristics

Fine-grained sedimentary rocks have undergone multiple processes such as sedimentation, diagenesis, and tectonism, to form a complex rock fabric. Rock structure, organic matter abundance, and mineral composition are the main components of the petrological characteristics of the organic-rich, fine-grained sedimentary rocks (Gong et al., 2017; Wu and Kong, 2025).

4.1.1 Rock structure

The structural types of sedimentary rocks are determined by the arrangement of mineral components. Based on the observations of cores and thin sections, the rock structures of fine-grained sedimentary rocks of the QFY Formation in the study area can be divided into three types: blocky, banded, and lamellar.

The blocky structure is the most common structure in the fine-grained sedimentary rocks of the QFY Formation in the NE Sichuan Basin. It is characterized by no significant changes in mineral composition and particle size, and the rock is homogeneous with a thickness generally greater than 2.5 cm. Different rock structures and lithologic combinations indicate different forming environments. Blocky claystone and blocky silty claystone are fine-grained sedimentary rocks dominated by clay minerals that are transported to deepwater areas far from the provenance, reflecting the semi-deep lake environment with weak hydrodynamics (Figures 2A, B). In contrast, siltstone, muddy siltstone, and shell limestone, which are rapidly deposited under strong hydrodynamics in shallow lakes, are generally blocky in structure and well sorted (Figures 2C, D).

Banded structures are parallel overlaps of alternately dark and bright banded on the core. The majority are horizontal, a few are wavy, and the thickness is greater than 0.5 cm and less than 2.5 cm. The formation of this structure in the study area is mainly related to the sudden increase of hydrodynamics in shallow water areas, such as terrigenous events including storms and turbidity currents (Figure 2E).

The lamellar structure in the study area can be divided into straight laminae and wavy laminae. The horizontal lamellar structure in lamellar silt-bearing claystone, lamellar silty claystone, and laminated claystone is a typical microrock structure of terrigenous hydrostatic sedimentary fine-grained sedimentary rocks (Figures 2F–I). It is formed in a low-energy environment with a warm and humid climate and semi-enclosed or closed water, representing the shallow lake and semi-deep lake environment with weak hydrodynamics. The wavy laminar structure indicates that the sedimentary water is relatively volatile, and it is speculated that the wavy laminae are formed in the shallow lake environment with shallow water and strong hydrodynamics.

4.1.2 Organic matter abundance

Statistically, the TOC content of the QFY Formation in the study area ranges from 0.12% to 3.71%, with an average of 1.85%. In the middle 2nd Member of the QFY Formation, the TOC content is the highest and gradually decreases vertically upward and downward. Compared with marine fine-grained sedimentary rocks, continental fine-grained sedimentary rocks are characterized by rapid sedimentary changes and a complex sedimentary environment. The development of organic-rich fine-grained sedimentary rocks is mainly controlled by the sedimentary environment with deepwater reduction.

4.1.3 Mineral composition

Whole-rock XRD analysis shows that the fine-grained sedimentary rocks of the QFY Formation in the study area are mainly composed of quartz, clay minerals, and carbonate minerals, with a small amount of feldspar, pyrite, siderite, and anhydrite. Overall, the content of clay minerals and quartz is high, and the carbonate minerals show local enrichment. It is observed that the quartz content in the analyzed samples varies from 8.7% to 60.9%, with an average value of 38.5%. Similarly, the clay content ranges from 19.4% to 66.6%, with an average of 48.9%, while the carbonate content ranges from 0.2% to 17.8%, with an average value of 2.3%. The clay minerals identified in the QFY Formation of the study area

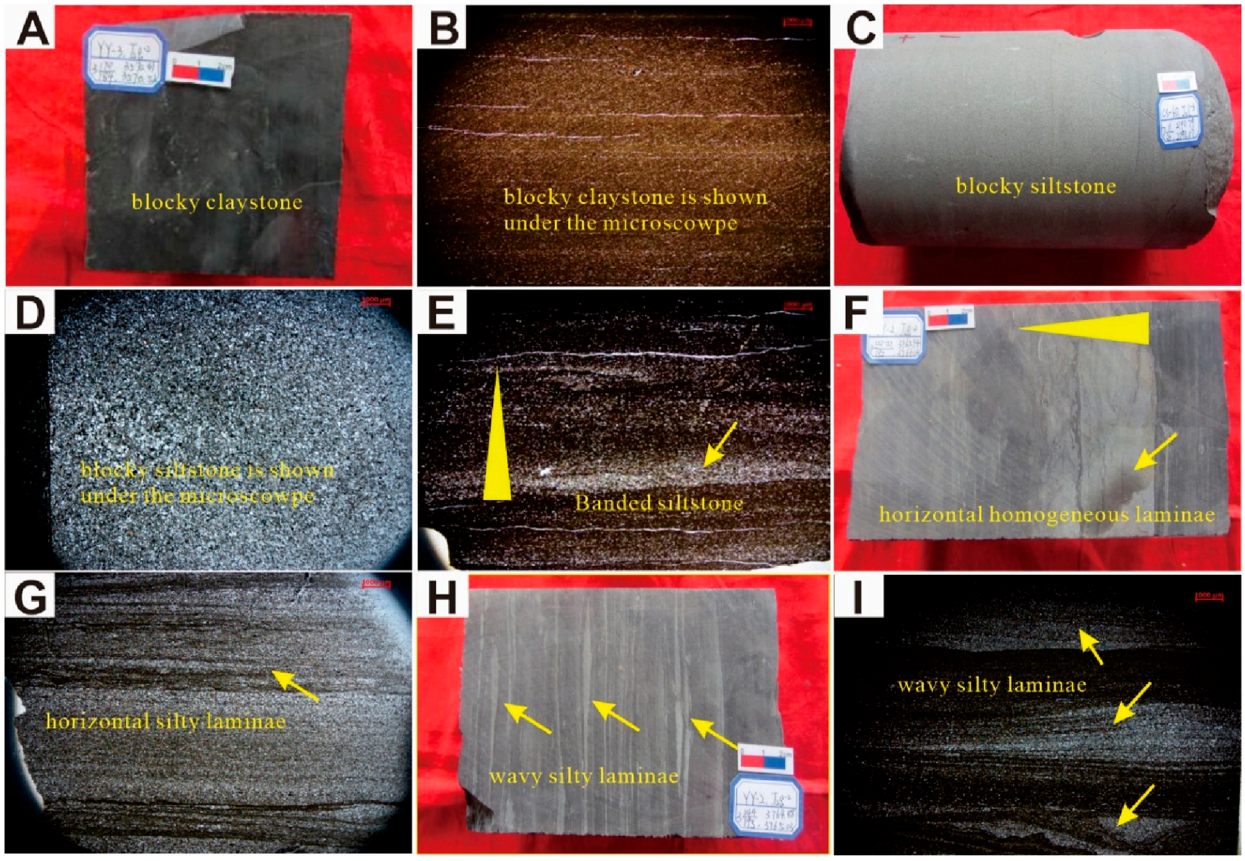

FIGURE 2
Different sedimentary structures of fine-grained sedimentary rocks in the QFY Formation. **(A)** Well YY3, 3570.52 m, 2nd Member, blocky claystone. **(B)** Well CS60, 2804.1 m, 2nd Member, blocky claystone. **(C)** Well CS60, 2792.79 m, 2nd Member, blocky siltstone. **(D)** Well YY3, 3556.16 m, 2nd Member, blocky siltstone. **(E)** Well LY1, 2779.7 m, 2nd Member, banding silty claystone. **(F)** Well YY2, 3725.94 m, 2nd Member, horizontal homogeneous laminae are developed. **(G)** Well YY3, 3603.06 m, 1st Member, horizontal silty laminae. **(H)** Well YY2, 3765.03 m, 2nd Member, wavy silty laminae. **(I)** Well YY3, 3523.98 m, 3rd Member, wavy silty laminae.

are illite, illite-smectite mixed layer, kaolinite, and chlorite. Notably, the highest content is observed for the illite-smectite mixed layer, which ranges from 28% to 55%, with an average of 42.48%, followed by illite, which ranges from 15% to 43%, with an average of 34%. The kaolinite content ranges from 2% to 35%, with an average of 6.39%, while the chlorite content ranges from 11% to 26%, with an average of 17% (Figure 3; Table 1).

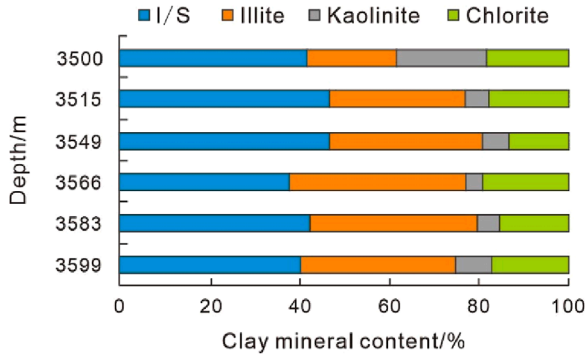

FIGURE 3
Percentage composition of clay minerals in the QFY Formation.

4.2 Reservoir physical properties

The shale gas exploration wells in the study area have a daily gas production of 0.71 × 10^4 m^3 and a daily oil production of 3 t in the fine-grained sedimentary rocks of the QFY Formation. To date, the cumulative gas production has reached 260.84 × 10^4 m^3 and the cumulative oil production has reached 2676.5 t. According to the test and analysis of the gas-bearing property for shale, the gas content of the fine-grained sedimentary rocks of the QFY Formation ranges from 0.25 m^3/t to 1.98 m^3/t, with an average of 1.03 m^3/t, and the gas-bearing property is quite good (the gas content is more than 1.00 m^3/t). The highest gas content is in organic-rich black blocky claystone (TOC is greater than 1.50%), grayish-black blocky silty claystone, and grayish-black laminated silty claystone, which range from 0.60 m^3/t to 1.98 m^3/t, with an average of 1.61 m^3/t (Figure 4).

The physical property tests of the core in the QFY Formation show that the porosity of black blocky claystones is between 0.4%

TABLE 1 XRD results of the clay minerals in the QFY Formation.

Sample number	Stratum	Depth/m	Relative content of clay minerals/%			
			Illite–smectite mixed layer	Illite	Kaolinite	Chlorite
1	QFY Formation	3505.16	55	25	6	14
2		3508.83	28	15	35	22
3		3510.17	46	30	4	20
4		3511.55	54	25	8	13
5		3514.78	53	29	2	16
6		3516.15	44	29	5	22
7		3518.26	37	32	5	26
8		3523.48	51	29	8	12
9		3526.59	48	31	6	15
10		3527.04	38	35	6	21
11		3529.2	49	33	4	14
12		3533.82	52	34	3	11
13		3539.02	46	30	13	11
14		3541.42	37	40	5	18
15		3545.43	43	35	5	17
16		3555.38	52	34	5	11
17		3558.66	34	43	4	19
18		3561.70	43	35	4	18
19		3562.51	34	40	3	23
20		3563.65	41	42	3	14
21		3565.10	37	36	6	21
22		3566.40	38	38	4	20
23		3569.51	32	41	5	22
24		3571.48	42	40	3	15
25		3574.66	52	32	5	11
26		3579.82	37	37	8	18
27		3583.15	41	39	4	16
28		3585.03	38	43	3	16
29		3602.55	42	32	6	16
30		3603.80	45	33	6	16
31		3605.33	28	39	14	19

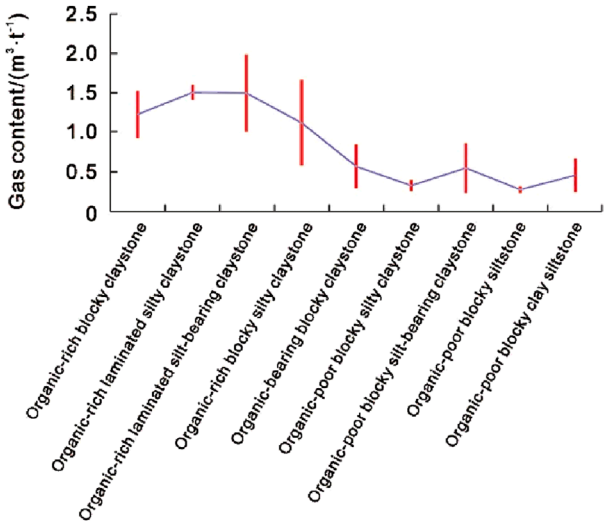

FIGURE 4
Gas-bearing test diagram of each lithofacies in the QFY Formation.

and 5.1%, with an average of 2.2%, and the permeability is between 0.004×10^{-3} μm^2 and 11.90×10^{-3} μm^2, with an average of 2.992×10^{-3} μm^2. The porosity of the grayish-black laminated silty claystone is between 0.6% and 3.3%, with an average of 1.9%, and the permeability is between 0.002×10^{-3} μm^2 and 0.689×10^{-3} μm^2, with an average of 0.289×10^{-3} μm^2. The porosity of the blocky silt-bearing claystone ranges from 1.0% to 4.8%, with an average of 3.2%, and the permeability is 0.144×10^{-3} μm^2 and 0.38×10^{-3} μm^2, with an average of 0.265×10^{-3} μm^2. According to the definition standard of the geological evaluation method for shale gas (GB/T 31,483–2015), the organic-rich continental shale in the semi-deep lake subfacies of the Middle Jurassic QFY Formation in the LZ-YB area, northeastern Sichuan Basin, satisfies the following conditions: the porosity, permeability, and TOC are greater than 2%, 0.1 × 10–^{3} μm^2, and 1%, respectively, and meet the standard of minimum industrial gas flow rate for continental shale gas (daily gas production is greater than 5,000 m^3), indicating that the fine-grained sedimentary reservoir in the QFY Formation can be used as a good reservoir.

4.3 Reservoir space types and characteristics

A total of 87 core samples of fine-grained sedimentary rocks in the QFY Formation from several coring wells in the study area were observed by argon ion polishing SEM. The examination of fine-grained sedimentary rocks under a microscope identified five distinct types of pores: silty intergranular pores, interlayer pores in clay minerals, intragranular pores in pyrite, organic matter-hosted pores, and microfractures.

4.3.1 Silty intergranular pores

Silty intergranular pores are one of the most common pores in the fine-grained sedimentary rocks of the QFY Formation in the study area. Because the LZ-YB area in the northeastern Sichuan Basin is close to the provenance of the Micangshan-Dabashan in the northern Sichuan Basin, the fine-grained sedimentary rocks are mixed with some silty sediments from the continental crust. These silty particles of terrigenous debris are dispersed in the shale. The intergranular pores are developed at the contact zones of mineral particles, but are affected by the shape of the detrital grains and the surrounding clay minerals. In particular, the silty intergranular pores formed by the dissolution of clay minerals and carbonate minerals are mostly irregular and pore-shaped. Some intergranular pores are distributed at the edges of brittle minerals such as quartz and feldspar grains, and the morphology of brittle minerals can also be seen through the distribution of intergranular pores (Figure 5A). In general, the porosity and permeability of brittle minerals are poor, and the pores are mostly filled with organic matter. Because of the influence of compaction and cementation in the diagenetic process, especially in the early diagenetic stage, a large number of intergranular pores are compressed and filled, resulting in relatively poor connectivity between pore throats.

4.3.2 Interlayer pores in clay minerals

According to the XRD analysis of clay minerals of rock samples in the QFY Formation, the content of illite–montmorillonite mixed layer is the highest in clay minerals of fine-grained sedimentary rocks of the QFY Formation in the study area, followed by illite, a small amount of kaolinite and chlorite, and montmorillonite is not developed. The illite–smectite mixed layer is the transitional mineral from montmorillonite to illite, which is honeycomb-shaped and flocculent. The illite is scaly and feathery, scattered on the surface of other mineral particles and filled between particles in the form of clay bridges. The morphology of these two clay minerals is mainly schistose. It gives the interlayer pores in the clay minerals in the study area a generally strong directionality and makes them show a parallel distribution and lamellar distribution with the cleavage plane of the clay minerals (Figure 5B). The interlayer pores can be filled by pyrite and organic matter (Chen et al., 2013). The grain boundary microfractures developed along the surface of clay minerals are mostly long banding. The long axis of the pores is generally between 10 nm and 50 nm, and the short axis is usually less than 1 μm. Due to the poor compressive resistance of clay minerals, the interlayer pores in clay minerals are sometimes curved under the influence of compaction in the early diagenetic stage. Because of the high content of clay minerals in fine-grained sedimentary rocks, the interlayer pore in clay minerals is the main pore type of the QFY Formation continental fine-grained sedimentary rocks in the study area, and its proportion is higher than that of other pores.

4.3.3 Intragranular pores in pyrite

Pyrite is formed in an anoxic reducing environment, and it is nodular-shaped and banded bedding or in a dispersed distribution in claystone and silty claystone. Pyrite is mainly developed in the form of framboidal aggregates in the fine-grained sedimentary rocks of the QFY Formation in the LZ-YB area (Figure 5C). Because the crystals are compacted, the spherical framboidal aggregates are formed. The aggregate diameters range from several microns to tens of microns. The pore size of the intragranular pores in the aggregates is large, approximately 10–80 nm. There are usually clay minerals or organic matter among framboidal pyrite, and the intragranular

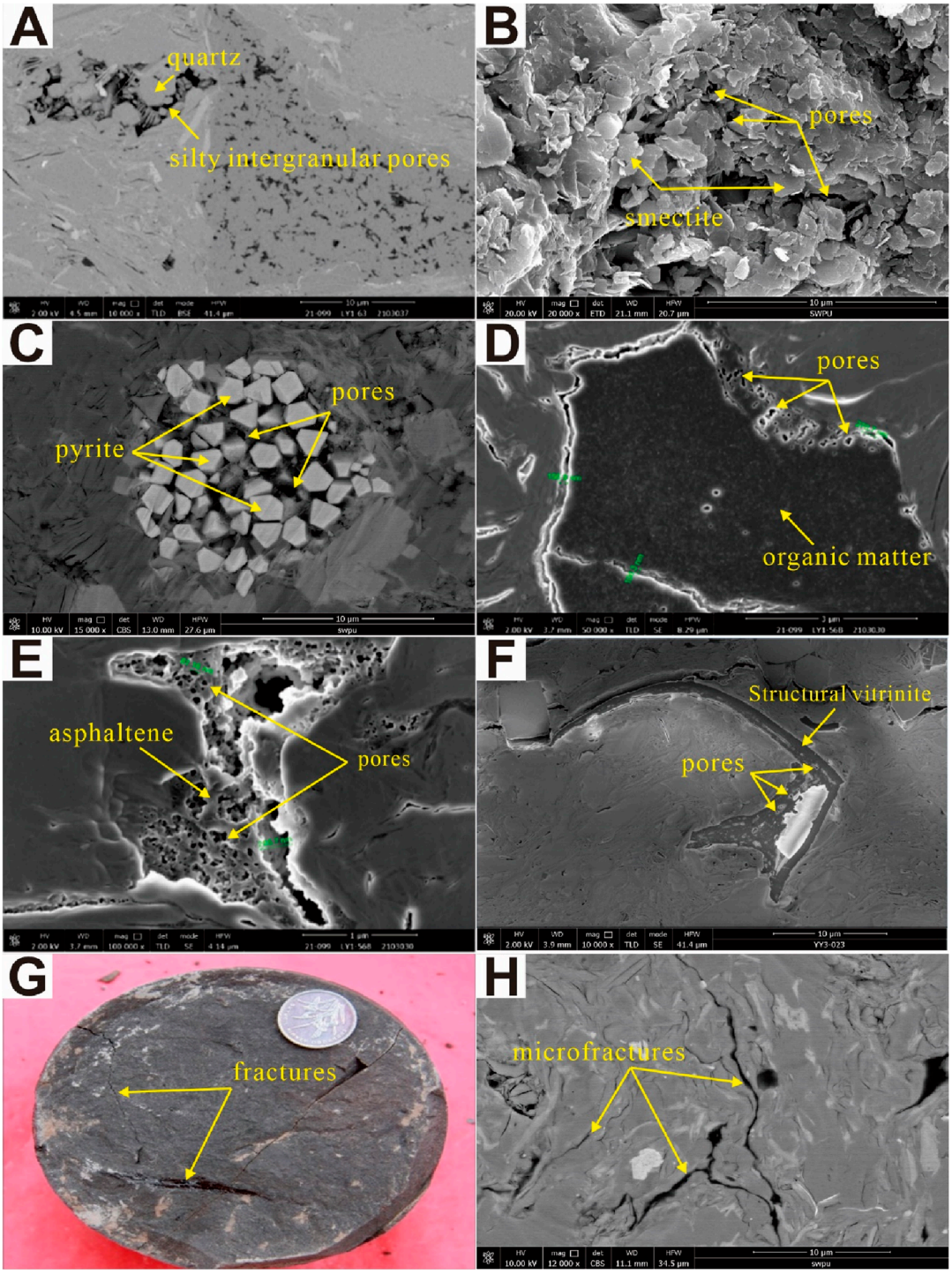

FIGURE 5
Pore characteristics of fine-grained continental sedimentary rocks in the QFY Formation. **(A)** Well LY1, 2746.36 m, 2nd Member, residual silty intergranular pores filled with quartz (SEM). **(B)** Well LY1, 2800.89 m, 2nd Member, smectite is distributed in sheets, and the pores between them have strong orientation (SEM). **(C)** Well YL4, 3647.14 m, 1st Member, intercrystalline pores in framboidal pyrite (SEM). **(D)** Well LY1, 2780.93 m, 2nd Member, scattered pores are developed around organic matter (SEM). **(E)** Well LY1, 2781.15 m, 2nd Member, pores are honeycomb-shaped (SEM). **(F)** Well YY3, 3518.26 m, 2nd Member, pores are developed in structural vitrinite (SEM). **(G)** Well LY1, 2785.46 m, 2nd Member, several fractures are developed with irregular surface and different widths, which are filled with asphaltene (photograph); **(H)** Well LY1, 2937.65 m, 1st Member, microfractures are developed (SEM).

pores in pyrite are easily blocked by surrounding organic matter or authigenic clay minerals.

4.3.4 Organic matter-hosted pores

Organic matter-hosted pores are usually formed in the process of hydrocarbon generation and exist within organic particles (Borjigin et al., 2021; Li H et al., 2022). The pore sizes of organic matter-hosted pores in the fine-grained sedimentary rocks of the QFY Formation in the study area are mainly nanoscale, with a diameter of approximately 30–50 nm, and the overall connectivity is poor. Two types of organic matter-hosted pores can be seen using SEM. One is in dispersed distribution with the organic matter filling in the silty intergranular pores as the main carrier (Figure 5D). Another is the honeycomb-shaped irregular oval or round hole (Figure 5E), with asphalt filled in microfractures as the main carrier, which is the main place for shale oil and gas preservation. The organic matter-hosted pores in fine-grained sedimentary rocks in the study area, observed by argon-ion-polishing SEM, are developed in the structural vitrinite (Figure 5F), and the pores are not developed in the vitrodetrinite and inertrodetrinite. With increasing burial depth and the influence of compaction, the scale of organic matter-hosted pores increases from microns to nanometers. In addition, organic matter-hosted pores are produced with the generation of organic hydrocarbons. Therefore, its pore characteristics are related to the type of organic matter, TOC, and maturity.

4.3.5 Microfractures

Macroscopically, shale bedding fractures and bedding slip scratches can be seen through the core (Li et al., 2021; Li H et al., 2025). Small-scale inclined joints and high-angle fractures are locally developed, with a length of 3–30 cm, and some fractures are filled with oil bloom and asphalt (Figure 5G). However, irregular inclined joints develop in the siltstone, while vertical fractures develop relatively, with a length of 3–24 cm and a width of 0.2–2 mm. Argon ion polishing SEM reveals that microfractures are mainly developed between clay mineral grains, the margins of organic matter, and the margins of the shell (Figure 5H).

According to the MAPS, the content of silty intergranular pores, interlayer pores in clay minerals, and intragranular pores in pyrite is the highest among all types of pores in continental fine-grained sedimentary rocks in the study area, followed by microfractures, and the content of organic matter-hosted pores is the lowest at less than 10%. (Figure 6).

5 Discussion

The QFY Formation in the study area is predominantly a shallow lacustrine to semi-deep lake sedimentary system. Within this system, semi-deep lacustrine subfacies claystones rich in organic matter and silty claystones are extensively developed, serving as the primary reservoir rock types for fine-grained sedimentary reservoirs. The influence of sedimentation on the fine-grained sedimentary rock reservoirs in the QFY Formation is mainly reflected in the following three aspects: (1) sedimentary facies control the enrichment of organic matter within fine-grained sedimentary rocks; (2) sedimentary facies dictate the types of rock structures that form fine-grained sedimentary rocks; and (3) sedimentary facies influence the mineral composition, thereby determining the distribution and development of different lithofacies within the fine-grained sedimentary rocks. Based on previous research methods, this paper comprehensively analyzed the effects of organic content, mineral composition, rock structure, sedimentary environment, and diagenesis on the reservoir quality of continental fine-grained sedimentary rocks in the study area.

5.1 Relationship between organic matter content and reservoir quality

According to previous studies, the organic matter content in fine-grained sedimentary rocks is closely related to the development of organic matter-hosted pores (Jiang et al., 2023; Zhou et al., 2025). The scatter plot conducted on the fine-grained sedimentary rocks in the studied region revealed a positive correlation between the TOC content and porosity (Figure 7). Furthermore, the results of the nano-CT experiment showed that the developing degree of organic matter-hosted pore development is positively associated with the content of organic matter and clay minerals (Aljamaan et al., 2017; Radwan et al., 2022; Wang B et al., 2023). With the increase of TOC and clay mineral content, the better the connectivity of shale pores and the higher the porosity.

5.2 Relationship between rock structure and reservoir quality

It is believed that natural microfractures are easily developed in lamellar and layered lithofacies (Gale et al., 2014; Wang and Wang, 2021; Li J et al., 2022; Liu G. Y et al., 2024). The porosity test results of more than 470 samples of the QFY Formation in the study area showed the following rules: the porosity of lamellar lithofacies was the highest, ranging from 1.3% to 5.9%, with an average of 4.0%. The porosity of banded lithofacies was the second, ranging from 1.0% to 4.8%, with an average of 2.7%, while the porosity of massive lithofacies was relatively low, ranging from 0.4% to 4.2%, with an average of 1.5% (Table 2).

According to the capillary pressure tested by the mercury intrusion method, the reservoir properties of lithofacies with different rock structures are different from each other (Luo et al., 2003; Yuan et al., 2016). The maximum connected pore throat radius of lamellar lithofacies was found to be between 0.011 μm and 0.148 μm with an average of 0.049 μm, and the median pore throat radius was found to be between 0.004 μm and 0.021 μm, with an average of 0.008 μm; the maximum connected pore throat radius of banded lithofacies ranged from 0.021 μm to 0.041 μm, with an average of 0.028 μm, and the median pore throat radius ranged from 0.004 μm to 0.006 μm, with an average of 0.005 μm; the maximum connected pore throat radius of massive lithofacies was found to be between 0.016 μm and 0.034 μm, with an average of 0.027 μm, and the median pore throat radius was found to be between 0.003 μm and 0.006 μm, with an average of 0.004 μm (Table 3). Comparing the three lithofacies, the lamellar lithofacies was found to have the largest maximum connected pore throat radius and the largest average pore throat radius, indicating that its lower limit of effective

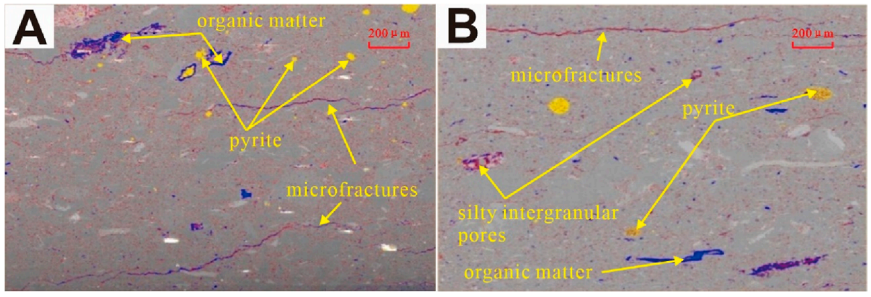

FIGURE 6
Void content analysis of fine-grained sedimentary rocks in the QFY Formation by macro-area backscatter imaging (MAPS). The pores are dominated by silty intergranular pores and microfractures between mineral particles (red is pores, blue is organic matter, and yellow is pyrite). **(A)** Well YY3, 3518.26 m, 2nd Member. **(B)** Well YY3, 3566.40 m, 2nd Member.

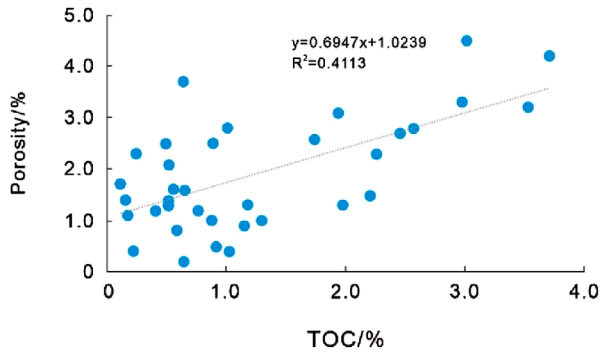

FIGURE 7
Relationship between TOC content and porosity.

TABLE 2 Porosity comparison of fine-grained sedimentary reservoirs with different rock structures.

Area	Well	Major lithofacies types	Porosity/%
LZ	LY1	Blocky claystone	0.40–2.50/1.35
		Banding silty claystone	1.00–3.10/1.80
		Blocky shell limestone	0.40–1.00/0.70
		Blocky siltstone	1.00–1.50/1.25
		Blocky clay siltstone	0.60–0.90/0.80
		Blocky silty claystone	0.60–1.40/1.00
		Laminated silt-bearing claystone	2.60–4.60/3.60
YB	YY3	Banding silty claystone	0.90–4.80/3.17
		Laminated claystone	4.10–5.10/4.60
		Blocky claystone	0.50–2.20/1.35
		Laminated silty claystone	3.20–5.90/4.83
		Blocky siltstone	0.90–1.50/1.20

pore throat radius was also the largest. From the perspective of mercury withdrawal efficiency, the numerical values of the lamellar facies and banded facies were significantly higher than those of the massive lithofacies, both of which were greater than 50%, indicating good reservoir connectivity. In general, the lamellar facies were found to have the best reservoir properties, followed by the banded lithofacies, while the massive lithofacies were found to have the worst reservoir properties.

5.3 Relationship between mineral composition and reservoir quality

The lithology of fine-grained sedimentary rocks of the QFY Formation in the study area can be classified into six types: claystone, silty claystone, silt-bearing claystone, siltstone, muddy siltstone, and shell limestone (Guo et al., 2014; Yang Y. M et al., 2022; Yang et al., 2023; He et al., 2023). The content of quartz in siltstones and muddy siltstones was found to be relatively high. Figures 8A–C show that the quartz content in fine-grained sedimentary rocks in the study area is negatively correlated with porosity, pore size, and pore volume. The higher the siliceous mineral content, the lower the reservoir space. Although quartz in fine-grained sedimentary rocks can increase the brittleness of fine-grained reservoirs, making them easier to fracture in the process of development, the main pores (intergranular pores) between the siliceous brittle particles are easily compressed and gradually decrease to non-existent during the burial process, indicating that the excessive siliceous minerals are not conducive to the development of pores (Zhang et al., 2020; Wan et al., 2025). According to the IUPAC classification standard, the curve of nitrogen adsorption has obvious hysteresis loops (Chen et al., 2023; Li J. J. et al., 2024). In the nitrogen adsorption experiment, the hysteresis loops of claystone, silt-bearing claystone, and silty claystone belong to H3 (Figure 9), reflecting the laminar pores. Because the clay minerals in the fine-grained sedimentary rocks of the QFY Formation in the study area were found to be dominated by the illite-smectite mixed layer and illite, the pores among the mineral compositions mainly composed of flaky particles mostly showed laminated features parallel to crystal structures under SEM. The pores with the laminated structure are beneficial in increasing

TABLE 3 Pore size comparison of fine-grained sedimentary reservoirs with different rock structures.

Well	Depth/m	Rock structure	Lithofacies types	Maximum connected pore throat radius/nm	Median pore throat radius/nm	Mercury removal efficiency/%
LY1	2810.81	Blocky	Blocky silty claystone	0.025	0.004	46.09
LY1	2790.66		Blocky claystone	0.034	0.005	30.17
LY1	2791.24		Blocky claystone	0.034	0.004	34.41
LY1	2793.78		Blocky claystone	0.031	0.005	33.17
YY3	3561.70		Blocky claystone	0.016	0.004	30.67
YY3	3566.40		Blocky silty claystone	0.024	0.004	34.53
YY3	3569.51		Blocky silty claystone	0.027	0.006	41.57
LY1	2807.40	Banding	Banding silty claystone	0.027	0.006	68.39
LY1	2794.68		Banding silty claystone	0.041	0.005	66.45
YY3	3585.74		Banding silty claystone	0.021	0.005	35.25
YY3	3606.43		Banding silty claystone	0.021	0.004	37.21
YY3	3562.51	Laminated	Laminated silt-bearing claystone	0.011	0.004	44.05
YY3	3563.65		Laminated silt-bearing claystone	0.013	0.004	71.57
YY3	3564.50		Laminated silty claystone	0.024	0.004	77.36
YY3	3538.24		Laminated silty claystone	0.148	0.021	76.95

the specific surface area of fine-grained sedimentary reservoirs and the adsorption of oil and gas.

It can be seen from Figures 8D–F that the clay mineral content in fine-grained sedimentary rocks in the study area is positively correlated with the volumes of micropores, mesoporous pores, and macropores, which indicates that with the increase of clay mineral content, the pores related to clay minerals are more developed in different pore sizes. Therefore, the clay minerals are the main controlling factor for the pore development of fine-grained sedimentary rocks in the QFY Formation in the LZ-YB area of the northeastern Sichuan Basin.

As can be seen from Figures 8G–I, there is no obvious correlation between carbonate mineral content and porosity, pore size, and pore volume.

5.4 Relationship between sedimentary environment and reservoir quality

5.4.1 Paleoredox environment

Jones and Manning (1994) drew the cross plot of the V/Cr and the degree of pyrite (DOP) in the Upper Jurassic mudstone in the Norwegian North Sea (Jones and Manning, 1994). Since then, other scholars have improved the accuracy of the V/Cr data points based on the analysis of the cross plot (Zhang et al., 2018). They believed that when V/Cr was less than 1.2, this was an indication of an oxidizing environment, while when V/Cr was more than 1.2, this indicated an anoxic–dysoxic environment. Combined with the theory by Hatch (Hatch and Leventhal, 1992), Zhang et al. (2018) studied the shale of the Wufeng–Longmaxi Formation in southeastern Chongqing, China, and found that when V/(V + Ni) was less than 0.46, this indicated an oxidizing environment; when the value ranged from 0.46 to 0.57, it indicated a weak oxidizing environment; if the value was observed to be between 0.57 and 0.83, it indicated an anoxic environment; and values between 0.83 and 1.00 indicated a euxinic environment. The value of V/Cr in the study area ranged from 1.22 to 1.54 with an average of 1.39, while the V/(V + Ni) ranged from 0.64 to 0.74 with an average of 0.71. These values reflect that in the sedimentary period, the QFY Formation in the study area was a sedimentary environment with an anoxic reducing condition. According to the scatter plot, V/Cr and V/(V + Ni) are positively correlated with specific surface area (S_{bet}) and total pore volume (V_{bjh}) (Figures 10A–D). The specific surface area of pores and pore volumes were observed to be larger in anoxic reducing conditions; in contrast, the two will shrink in oxygen-bearing oxidizing conditions. This shows that redox conditions can control the pore structures of the reservoir.

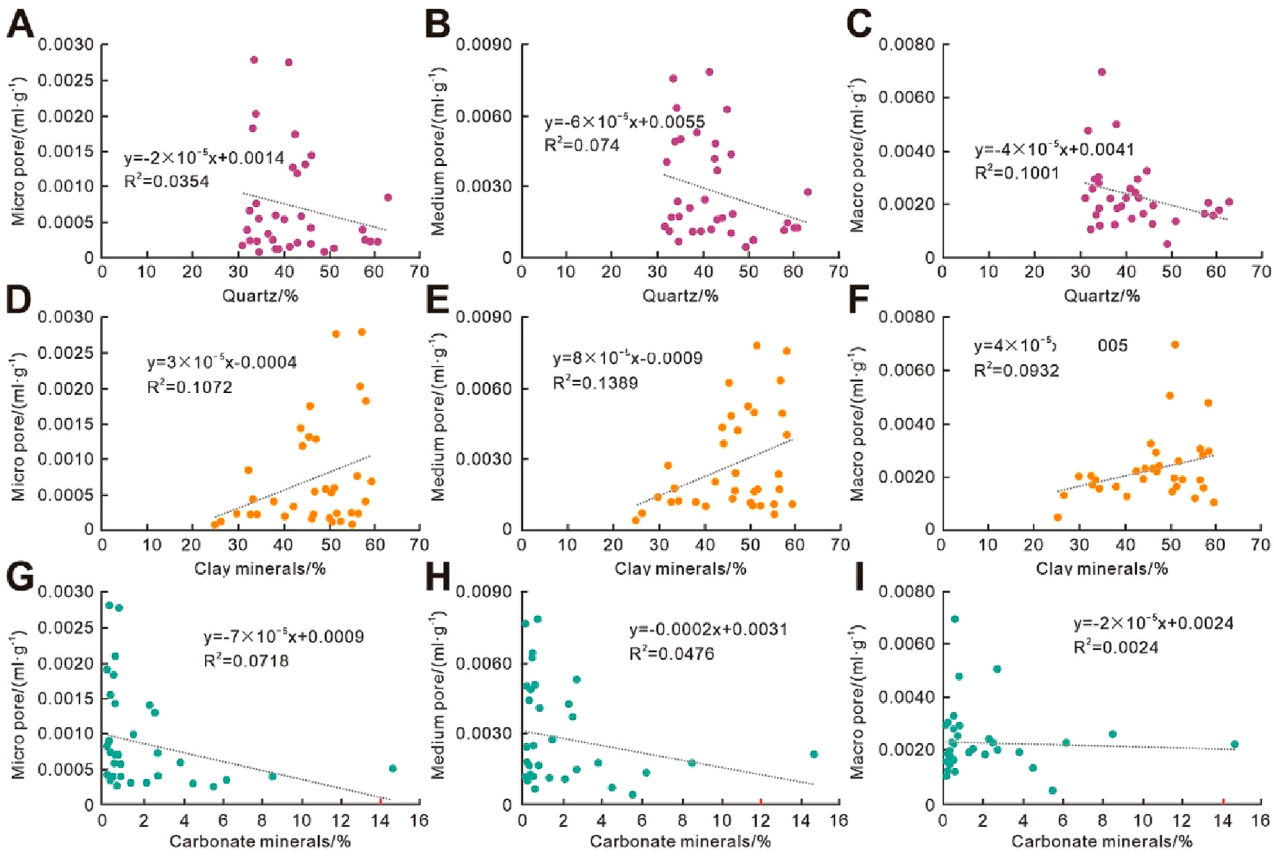

FIGURE 8
Correlation between pore volume and mineral content at different scales. **(A)** Relationship between quartz content and micropores. **(B)** Relationship between quartz content and middle pores. **(C)** Relationship between quartz content and macropores. **(D)** Relationship between clay mineral content and micropores. **(E)** Relationship between clay mineral content and middle pores. **(F)** Relationship between clay mineral content and macropores. **(G)** Relationship between carbonate mineral content and micropores. **(H)** Relationship between carbonate mineral content and medium pores. **(I)** Relationship between carbonate mineral content and macropores.

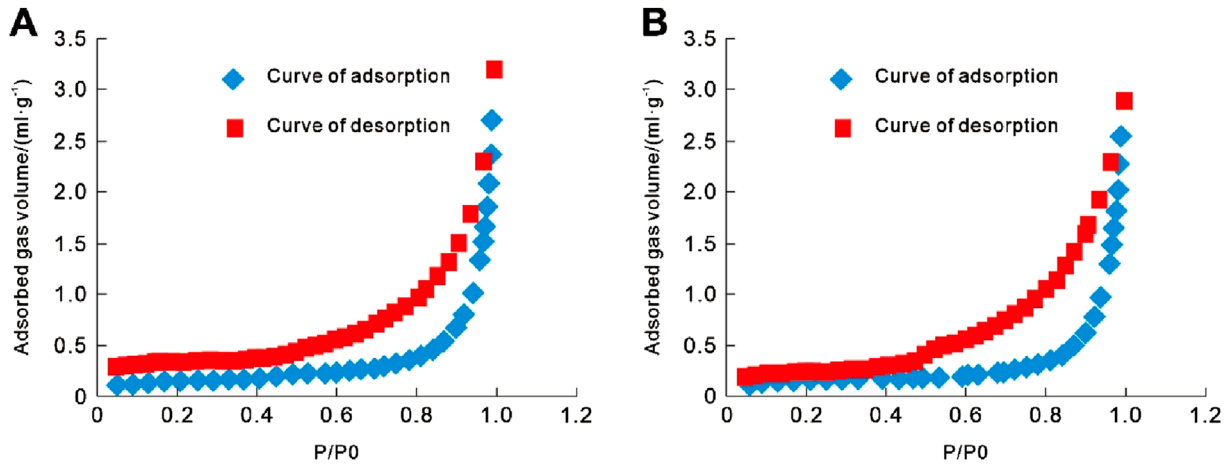

FIGURE 9
Nitrogen adsorption curve of claystone in the QFY Formation (P/P0: The ratio of gas pressure during adsorption to the vapor pressure at saturation, ranging from 0 to 1). **(A)** Well LY1, 2754.12 m, 2nd Member, claystone. **(B)** Well LY1, 2779.7 m, 2nd Member, silty claystone.

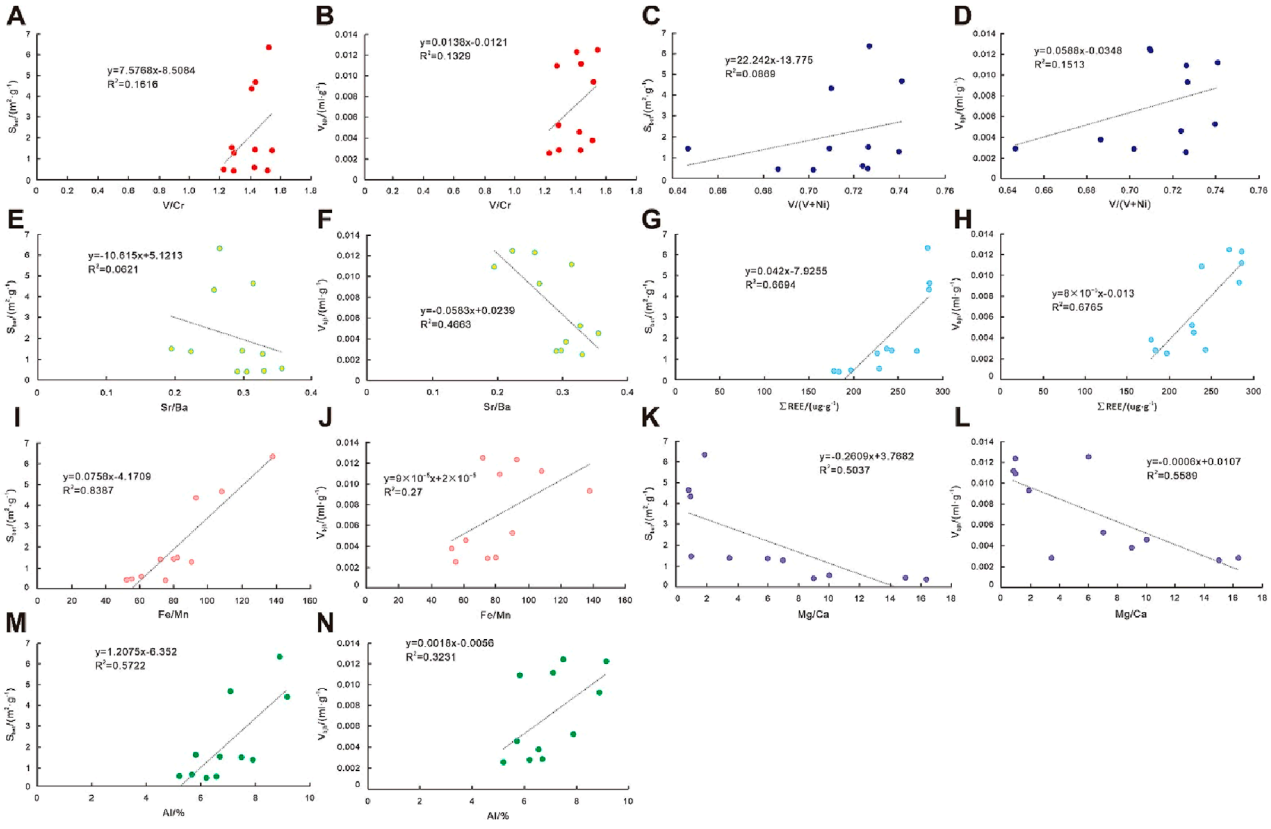

FIGURE 10
Relationships between geochemical indicators of different elements and specific surface area and total pore volume of the reservoir. **(A)** V/Cr vs. S_{bet}. **(B)** V/Cr vs. V_{bjh}. **(C)** V/(V + Ni) vs. S_{bet}. **(D)** V/(V + Ni) vs. V_{bjh}. **(E)** Sr/Ba vs. S_{bet}. **(F)** Sr/Ba vs. V_{bjh}. **(G)** ∑REE vs. S_{bet}. **(H)** ∑REE vs. V_{bjhs}. **(I)** Fe/Mn vs. S_{bet}. **(J)** Fe/Mn vs. V_{bjh}. **(K)** Mg/Ca vs. S_{bet}. **(L)** Mg/Ca vs. V_{bjh}. **(M)** Al vs. S_{bet}. **(N)** Al vs. V_{bjh}.

5.4.2 Paleosalinity

The value of Sr/Ba was used to determine the paleosalinity of sedimentary water in the QFY Formation, northeastern Sichuan Basin (Fu et al., 2023). The content of Sris relatively small in the freshwater zone, and the Sr/Ba is usually less than 1 in freshwater sediments, while the content of Sr increases correspondingly in saline-water sediments, and the Sr/Ba is greater than 1. The value of Sr/Ba in the study area ranged from 0.19 to 0.35, with an average of 0.28, indicating that in the sedimentary period, the QFY Formation in the LZ-YB area was a freshwater lake sedimentary environment. The value of Sr/Ba is negatively correlated with specific surface area (S_{bet}) and total pore volume (V_{bjh}) (Figures 10E, F). This indicates that the higher the salinity of the lake water, the smaller the reservoir space. Lake water with high salinity provides the material environment for the formation of shell limestone because the environment is suitable for the growth of lamellibranchiate organisms. With increasing carbonate content, it is easy for cementation to occur in the process of diagenesis blocking and filling pores and damaging the reservoir space.

5.4.3 Paleoclimate

According to the statistics, the total content of rare earth elements (∑REE) in the core samples of YL4 well in the study area was found to be approximately 237.68 μg/g, which is relatively high. This demonstrates the large terrestrial input and warm and humid climate in the sedimentary period. The ratios of two elements (Fe/Mn and Mg/Ca), which indicate paleoclimate, averaged 85.57 and 5.01, respectively, in the QFY Formation in the study area. Both high Fe/Mn and low Mg/Ca values reflect the warm and humid climate of the QFY Formation in the study area. The values of ∑REE and Fe/Mn are positively correlated with specific surface area (S_{bet}) and total pore volume (V_{bjh}), while the value of Mg/Ca is negatively correlated with them (Figures 10G–L). This means that the reservoir space in fine-grained sedimentary reservoirs develops more easily in warm and moist climates. A wetter climate will bring more precipitation, which will make the water level rise in the lake basin and the deepwater area enlarge (Falahatkhah et al., 2025). All these conditions facilitate the buildup of clay minerals and organic matter. The higher the content of clay minerals and organic matter in fine-grained sedimentary rocks, the more interlayer pores in clay minerals and organic matter-hosted pores, which makes it easier to form a better reservoir space.

5.4.4 Paleoproductivity

The content of the Al element in the study area was found to range from 5.82% to 9.15%, with an average of 7.05%, which indicates high paleoproductivity. By comparing the scatter plots,

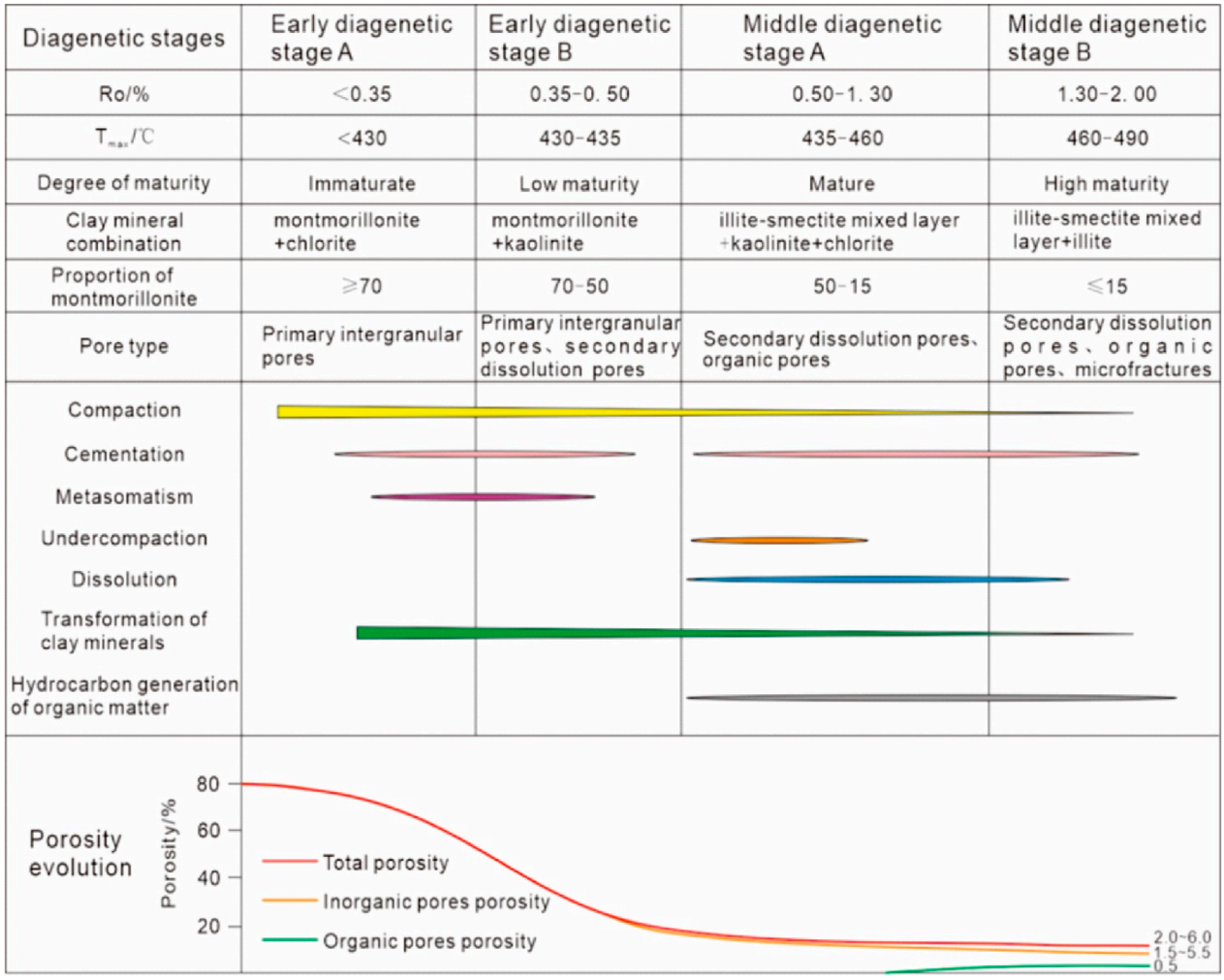

FIGURE 11
Diagenetic stage and diagenetic evolution of the reservoir.

it can be seen that the content of the Al element is positively correlated with the specific surface area (S_{bet}) and total pore volume (V_{bjh}) of the reservoir (Figures 10M, N). Because terrigenous debris can provide nutrients for organic matter production, the more terrigenous inputs into the lake basin, the more favorable it is for the formation of organic matter-hosted pores (Tan et al., 2024). The QFY Formation in the study area is in a warm climate during the sedimentary period, which is conducive to plant growth. The large runoff into the lake brought abundant terrestrial plants and nutrients to the lake basin; as a result, the aquatic plankton thrived, leading to an increase in the productivity of organic matter. With the rising organic matter content, organic matter-hosted pores also increased.

The reservoir space was found to be well developed in fine-grained sedimentary rocks formed in the sedimentary environment with anoxic reducing conditions, fresh water, wettability, and sufficient terrigenous debris. Therefore, the sedimentary environment of the QFY Formation in the study area was found to be one of the controlling factors of the reservoir space in continental fine-grained sedimentary rocks.

5.5 Relationship between diagenesis and reservoir quality

According to the oil and gas industry standard for the division of diagenetic stages in clastic rocks (SY/T 5477-2003), the continental fine-grained sedimentary rocks in the study area have entered the B phase of the middle diagenetic stage, which mainly experiences a series of diagenesis including compaction, cementation, dissolution, recompaction, clay mineral transformation, and the hydrocarbon generation from organic matter (Figure 11). Different diagenesis will constantly change the pore structure of fine-grained sedimentary reservoirs.

According to the intensity category of diagenesis, the compaction ratio in fine-grained sedimentary reservoirs in the study area mainly ranges from 21.3% to 83.6%, with an average of 60.5%, which is dominated by medium-strong compaction (Figure 12). This shows that fine-grained sedimentary rocks are greatly influenced by compaction, resulting in the shale bedding fractures dominated by lamellar fractures in the fine-grained sedimentary rocks that are strongly compressed and compacted. Under the function of stress,

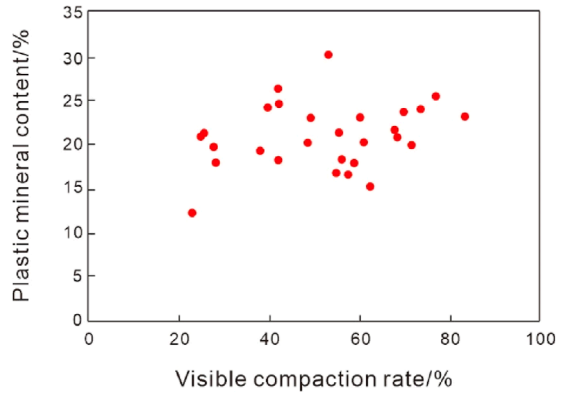

FIGURE 12
Relationship between plastic component content and compaction rate of fine-grained sedimentary reservoirs in the QFY Formation.

the particles in the sedimentary rocks show directional arrangement, and it can be seen that the lumachelles in shell limestone and shell mudstone are layered and overlapping. (Figure 13A).

The cast thin section, SEM, and X-ray diffraction studies of clay minerals show that there are mainly calcareous cementation and siliceous cementation, with a small amount of ferruginous cementation in fine-grained sedimentary reservoirs in the QFY Formation (Figures 13B, C). According to the Houseknecht evaluation method (Houseknecht, 1987), the porosity lost by cementation of fine-grained sedimentary reservoirs in the study area averages 16.55% (Figure 14). Overall, the influence of carbonate cement and siliceous cement on the pores of fine-grained sedimentary rocks is generally negative, and both dispersion and cementation will cause the reduction of the pores forming tight layers. Cementation is the main diagenesis resulting in poor reservoir properties in the study area.

In the study area, dissolution is developed in the carbonate minerals of the shell limestone and shell-bearing claystone, and the dissolution of calcite can be divided into early dissolution and late dissolution, with high intensity in the early stage. Carbonate minerals are easily dissolved by carbonate compounds, which are generated by the dissolution of carbon dioxide in water during the hydrocarbon generation process of organic matter, resulting in a certain number of secondary pores, such as intergranular dissolution pores (Figure 13D). XRD analysis of fine-grained sedimentary rocks in the QFY Formation shows that the content of calcite and dolomite is small, with an average of less than 3%. Therefore, carbonate minerals do not play an important role in the porosity evolution of fine-grained sedimentary reservoirs in the QFY Formation in the study area.

Although organic matter can provide material for organic matter-hosted pores, its content in continental shales cannot do much for organic matter-hosted pores. At the same time, the organic matter will occupy the development space of other pores. Therefore, the hydrocarbon generation of organic matter in continental fine-grained sedimentary rocks has little effect on improving reservoirs.

Zhao and Jin suggested that burial depth in the study area is generally greater than 2000 m (Zhao and Jin, 2021). When the formation temperature rises to 70°C–100°C, the rock has been completely consolidated under higher pressure, and the transformation among clay minerals is the main diagenesis in this period. Clay mineral X-ray diffraction results of core samples from several wells in the study area show that clay minerals basically do not contain montmorillonite but are dominated by illite and illite–smectite mixed layer (Figures 13E, F). This indicates that the montmorillonite or illite–smectite mixed layer in fine-grained sedimentary rocks will transfer into illite or illite–smectite mixed layer minerals with the increasing burial depth. The transformation of montmorillonite to illite is a spontaneous reaction with low energy consumption. The illite produced in this process is often in the form of irregular, tiny crystal plates and granular coatings, and the crystallinity improves with increasing burial depth. In the transformation process , montmorillonite precipitates interlayer water and structural water, causing the collapse of the crystal lattice and the shrinkage of the mineral particle volume, and forming a large number of interlayer pores in clay minerals. In addition, the pore volume also increases, which improves the adsorption capacity and reservoir space. With the increasing clay mineral transformation, many shale bedding fractures are formed, and clay laminae are developed. Compared with silt laminae, micro-nano pores and fractures are developed in the parts where clay laminae are developed, and the connectivity is relatively good, which effectively improves the reservoir capacity of fine-grained sedimentary rocks. In general, the clay minerals generated via transformation have the potential to augment the specific surface area of pores and enhance the oil and gas absorption capacity within fine-grained sedimentary reservoirs.

The recompaction merely develops in shale. The average of the acoustic time logging curve from the 2nd Member to the 1st Member in the QFY Formation (3500–3600 m) is close to the average of the curve near 2700–2800 m in the Lower Shaximiao Formation, which served as upper shallow strata. Both of them are greater than 80 μs/ft, which is obviously higher than the average of the acoustic time logging curve (less than 50 μs/ft) in the slow compaction area near 700 m from Lower Shaximiao Formation to the 3rd Member of the QFY Formation, which means that there is an overpressure area for the rocks in the shale section of the QFY Formation (Figure 15).

With the increasing burial depth and formation temperature, fine-grained sedimentary rocks are affected by mechanical and chemical compaction, and their internal sealing is enhanced, which makes solid organic matter mature into hydrocarbons. The fluid in the pores, with volume expansion and increased pressure, cannot be discharged in time and cannot bear the pressure from the overlying rock skeleton. The recompaction supports the internal pore structure of the fine-grained sedimentary rocks and preserves some pore structure in the rock.

Research shows that the fine-grained sedimentary reservoirs of the QFY Formation are dominated by unfilled to half-filled structural microfractures with good effectiveness (Figure 16). These microfractures can provide channels for the initial migration of oil and gas and storage space for organic matter-hosted pores. At the same time, the unstable components on both sides of the microfractures are broken under the action of pore water. Corrosion occurs along the edges of the broken particles, which results in secondary pores, increases rock porosity, and improves the physical properties of the reservoir. Microscopic observation of thin sections shows that a few of the microfractures in the reservoir are bifurcated.

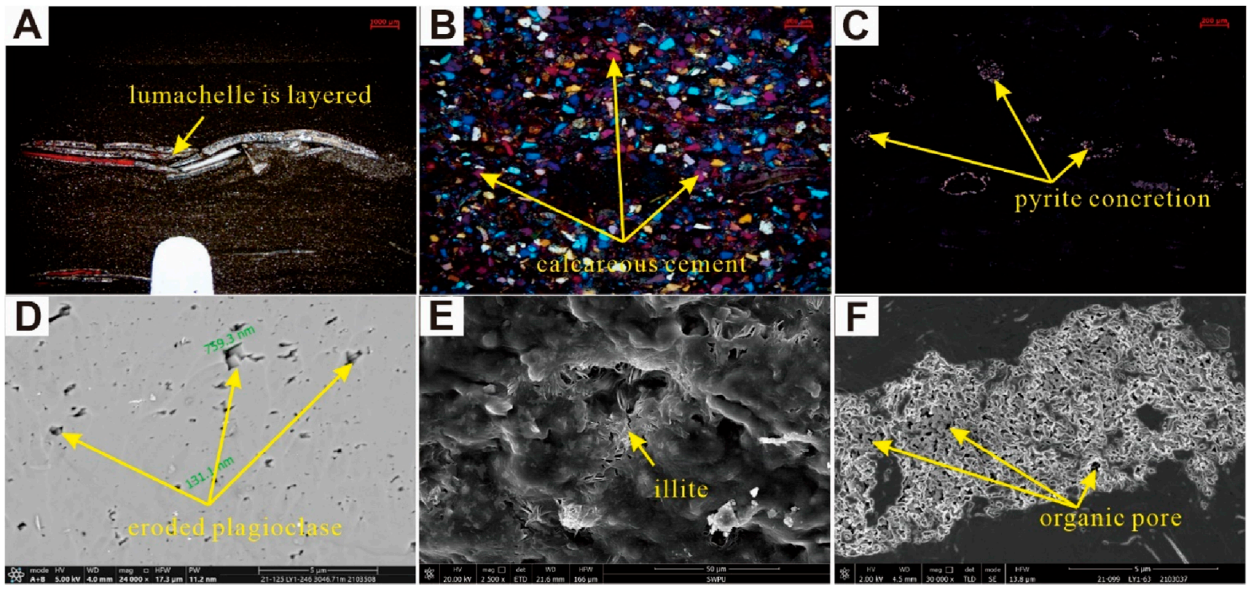

FIGURE 13
Characteristics of diagenesis in continental fine-grained sedimentary rocks in the QFY Formation. **(A)** Well YY3, 3609.28 m, 1st Member, the lumachelle is layered overlapping under compaction, 1X (–). **(B)** Well YY2, 3769.02 m, 2nd Member, the calcareous cement in siltstone, 5X (+). **(C)** Well YY2, 3777.56 m, 1st Member, the pyrite is an aggregated distribution, 10× (reflected light). **(D)** Well LY1, 2880.96 m, 1st Member, eroded plagioclase (SEM). **(E)** Well LY1, 2760.30 m, 2nd Member, clay minerals are transferred into illite (SEM). **(F)** Well LY1, 2784.67 m, 2nd Member, organic matter-hosted pores are developed in a complex of solid asphalt and the clay mineral kaolinite (SEM).

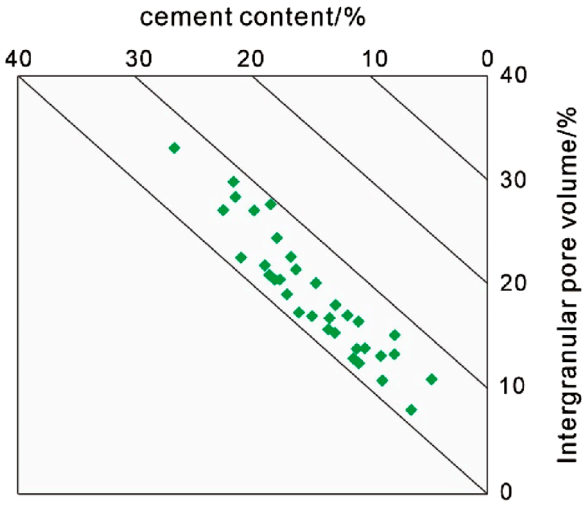

FIGURE 14
Relationship between cement and intergranular pore volume in fine-grained sedimentary reservoirs in the QFY Formation.

The bifurcated microfractures can connect other microfractures to form a complex network fracture system, which improves the seepage capacity of the reservoir to a certain extent and connects different reservoir spaces in the reservoir to form an aggregate of reservoir space. Thus, these microfractures formed by tectonism are the main filtrating channels for fluids in the reservoir and important storage space for oil and gas. During the later stages, when carrying out the fracture test production of oil and gas in fine-grained sedimentary reservoirs, the microfractures forming the fracture network also play an important and constructive role in the fracturing transformation of the reservoirs.

5.6 Implications for petroleum exploration and development

The abundance of organic matter is an important material basis for the formation of oil and gas in continental fine-grained sedimentary rocks, and the sedimentary environment can affect the burial and preservation of organic matter. In the semi-deep lake subfacies area, the water depth is deeper, the water is more reductive, the organic matter preservation conditions are better, and a set of fine sedimentary rocks with relatively large thickness and rich in organic matter and horizontal stratification can be deposited, such as claystones and silty claystones with good organic matter types, which provide the necessary material basis for oil and gas enrichment. The rock structure also has an important influence on oil and gas enrichment. The lamellar structure can not only affect the type of reservoir space, the distribution of pore size, and the development of pores and fractures but also control the porosity and permeability of the reservoir and greatly improve the horizontal seepage capacity of the reservoir. In this study, organic-rich laminar silty claystones develop a large number of laminar structures. Due to the different mineral properties in different laminates, many bedding fractures and mineral shrinkage fractures develop in the laminar segments, which are favorable spaces for oil and gas accumulation. Among them, bedding fractures are effective reservoir spaces and seepage

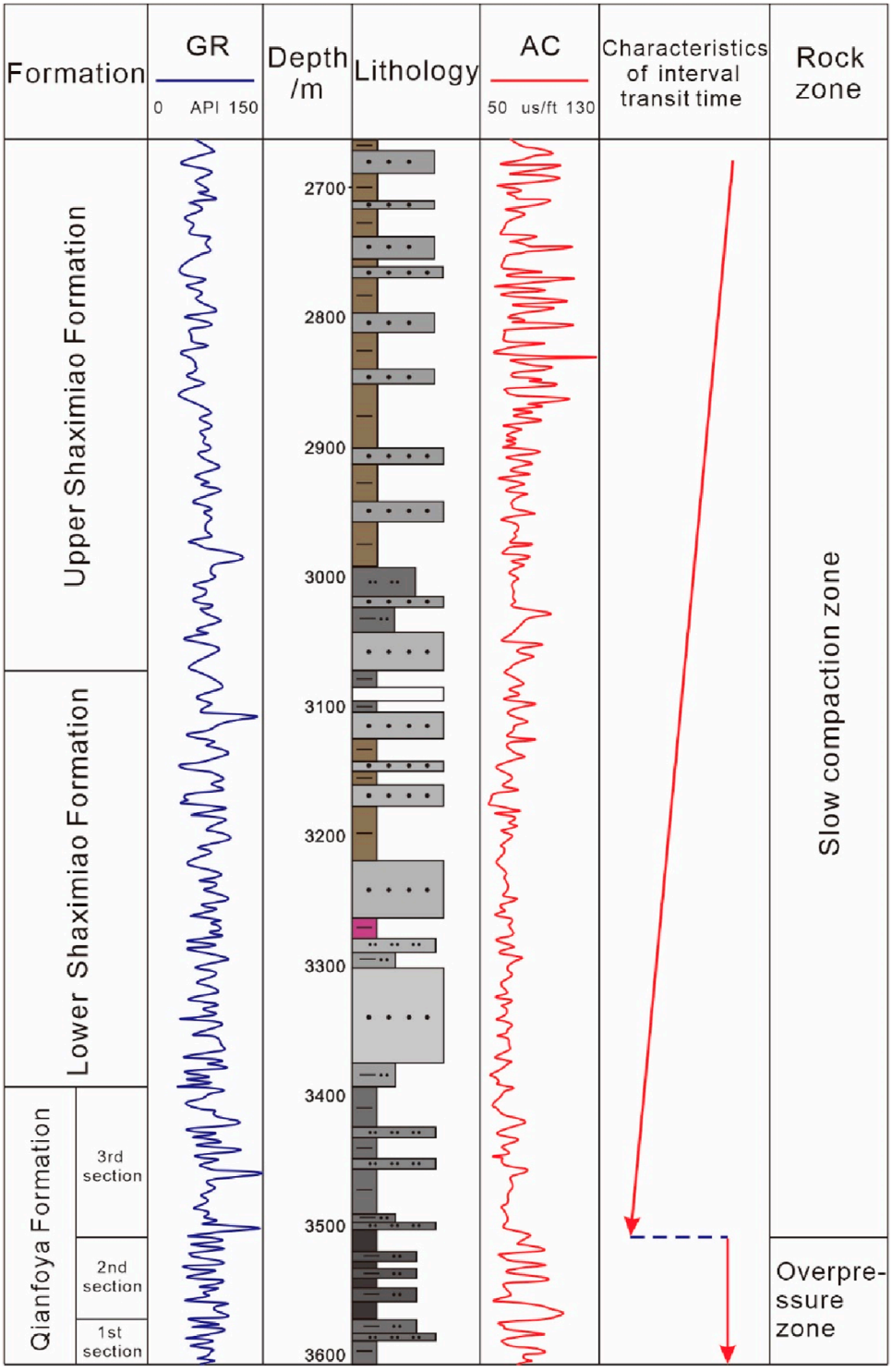

FIGURE 15
Characteristics of the undercompaction section in well YY3 (from 3500 m to 3600 m, the fine-grained sedimentary rocks from the 2nd to the 1st Member of the QFY Formation are an overpressure zone).

channels that affect the accumulation of oil and gas and the productivity of individual wells. Different mineral compositions also have an impact on oil and gas enrichment. Because the clay minerals in the fine-grained sedimentary rocks of the QFY Formation in the study area are mostly illite–smectite mixed layer and illite, the pores between the mineral compositions dominated by flake particles are mostly layered parallel to the crystal structure under scanning electron microscopy. The pore of this layered structure is

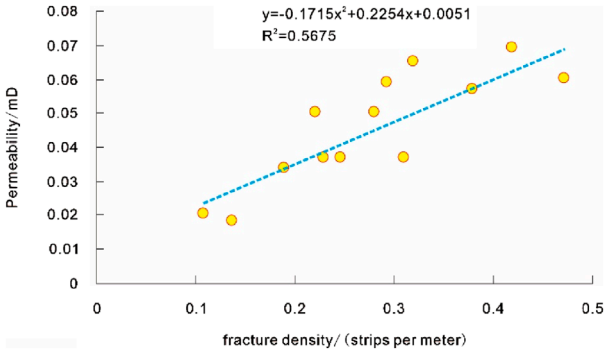

FIGURE 16
Relationship between tectonic fracture density and reservoir permeability.

conducive to increasing the specific surface area of the fine-grained sedimentary rock reservoir and is also conducive to the adsorption of oil and gas.

Overall, the continental fine-grained sedimentary rocks of the QFY Formation in the LZ-YB area have considerable oil and gas resource potential. By discussing the main controlling factors of oil and gas enrichment, the efficiency of oil and gas exploration and development of continental fine-grained sedimentary rocks in northeast Sichuan will be greatly improved.

6 Conclusion

(1) The fine-grained sedimentary rocks in the QFY Formation in the LZ-YB area, northeastern Sichuan Basin, mainly develop three rock structures. They are blocky, banded, and lamellar structures. The middle part of the 1st Member of the QFY Formation is a better source rock among the continental fine-grained sedimentary rocks whose TOC content is high, with an average of 1.85%. It also has a high potential for hydrocarbon generation. The mineral composition is dominated by clay minerals and felsic minerals, while the content of carbonate minerals is low. The clay minerals are mainly composed of illite and illite-smectite mixed layers.

(2) The porosity, permeability, TOC, and daily gas production of the organic-rich continental fine-grained sedimentary rocks of the semi-deep lacustrine subfacies of the QFY Formation in the LZ-YB area, northeastern Sichuan Basin, are greater than 2%, 0.1×10^{-3} μm^2, 1%, and 5 million cubic meters, respectively. All of them meet the standard of the minimum industrial gas flow rate for the continental shale gas; thus, it can be regarded as a good reservoir.

(3) According to the genesis of the reservoir space in continental fine-grained sedimentary rocks, the reservoir space identified from the fine-grained sedimentary rocks in the QFY Formation can be divided into silty intergranular pores, interlayer pores in clay minerals, intragranular pores in pyrite, organic matter-hosted pores, and microfractures. In the reservoir space, the proportion of silty intergranular pores is the highest, followed by interlayer pores in clay minerals and microfractures, a small number of intragranular pores exist in the strawberry-shaped pyrite, while the proportion of organic matter-hosted pores is less than 10%.

(4) The reservoir quality of continental fine-grained sedimentary rocks is controlled by multiple factors such as organic content, mineral composition, rock structure, sedimentary environment, and diagenesis. The claystone, which is rich with organic matter, horizontal laminae, and silt-bearing claystone, provides the material foundation for reservoirs with good reservoir properties and connectivity. The sedimentary environment with anoxic reducing conditions, fresh water, wettability, and sufficient terrigenous debris is conducive to the development of pore space in fine-grained sedimentary rocks. During the diagenetic process, the improvement of reservoir quality is mainly influenced by clay mineral transformation and recompaction, and the pores formed by clay mineral transformation are well preserved under recompaction. Microfractures formed by tectonism are the main filtration channels of fluids in the reservoir and an important reservoir space of oil and gas. They play an important role in the fracturing transformation of the reservoir.

Data availability statement

The original contributions presented in the study are included in the article/supplementary material; further inquiries can be directed to the corresponding author.

Author contributions

LC: conceptualization, data curation, formal analysis, investigation, methodology, software, writing – original draft, and writing – review and editing. JP: conceptualization, funding acquisition, project administration, resources, supervision, validation, and writing – review and editing.

Funding

The author(s) declare that financial support was received for the research and/or publication of this article. The 2025 Central University Basic Scientific Research Business Expense Support Project - Doctoral Innovation Capacity Enhancement Project, Project Number: 25CAFUC04059.

Conflict of interest

The authors declare that the research was conducted in the absence of any commercial or financial relationships that could be construed as a potential conflict of interest.

Generative AI statement

The author(s) declare that no Generative AI was used in the creation of this manuscript.

Publisher's note

References

Aljamaan, H., Ross, C. M., and Kovscek, A. R. (2017). Multiscale imaging of gas storage in shales. *SPE J.* 22 (6), 1760–1777. doi:10.2118/185054-PA

Bian, R. K. (2024). The formation and evolutionary characteristics of organic matter and pyrites in the continental shales of the 3rd submember of Chang 7 Member, Yanchang formation, Ordos Basin, China. *Energy Geosci.* 5 (2), 100250. doi:10.1016/j.engeos.2023.100250

Borjigin, T., Lu, L. F., Yu, L. J., Zhang, W. T., Pan, A. Y., Shen, B. J., et al. (2021). Formation, preservation and connectivity control of organic pores in shale. *Petrol. explor. Dev.* 48 (4), 798–812. doi:10.1016/S1876-3804(21)60067-8

Chen, L. X. (2022). A study on the inhomogeneous sedimentation-diagenesis-reservoir formation mode of deep tight marine clastic rock reservoirs in the Silurian Xiaoheba Formation, southeast Sichuan. *Front. Earth Sci.* 10, 900188. doi:10.3389/feart.2022.900188

Chen, W. L., Zhou, W., Luo, P., Deng, H. C., Li, Q., Shan, R., et al. (2013). Analysis of the shale gas reservoir in the lower silurian Longmaxi Formation, changxin 1 well, southeast Sichuan Basin, China. Acta petrol. *Sin.* 29 (3), 1073–1086.

Chen, Y. N., Yang, K., Wu, W., Yang, Y. R., Yang, X., and Ma, K. (2023). Favorable lithofacies and pore characteristics of the permian longtan formation shale in the southern Sichuan Basin. *Energy Geosci.* 4 (3), 100193. doi:10.1016/j.engeos.2023.100193

Dai, Q. Q., Luo, Q., Zhang, C., Lu, Z. J., Zhang, Y. Z., Lu, S. J., et al. (2016). Pore structure characteristics of tight-oil sandstone reservoir based on a new parameter measured by NMR experiment: a case study of seventh Member in Yanchang Formation, Ordos Basin. *Acta Petrol. Sin.* 37 (7), 887–897. doi:10.7623/syxb201607007

Dong, S. Q., Zeng, L. B., Wang, L. T., Lyu, W. Y., Xu, H., Ji, C. Q., et al. (2024). Fracture identification in shale reservoir using a deep learning method: Chang 7 reservoirs, Triassic Yanchang formation. *Geoenergy Sci. Eng.* 238, 212853. doi:10.1016/j.geoen.2024.212853

Falahatkhah, O., Ghaderi, A., Kadkhodaie, A., and Rezaee, R. (2025). Milankovitch-driven terrigenous deposit influx in Middle Ordovician marine successions of Western Australia: insights for paleoclimate and geochronology. *Mar. Petrol. Geol.* 173, 107282. doi:10.1016/j.marpetgeo.2024.107282

Fan, C. H., Li, H., Qin, Q. R., He, S., and Zhong, C. (2020). Geological conditions and exploration potential of shale gas reservoir in Wufeng and Longmaxi Formation of southeastern Sichuan Basin, China. *J. Petrol. Sci. Eng.* 191, 107138. doi:10.1016/j.petrol.2020.107138

Fu, Q., Hu, Z. Q., Feng, D. J., Huang, J. L., Xing, L. L., Zhu, Z. W., et al. (2023). Restoration and evolution of the Paleogene (E1f2) shale sedimentary environment in the Subei Basin, China. *ACS Omega* 8 (49), 46892–46903. doi:10.1021/acsomega.3c06603

Gale, J. F. W., Laubach, S. E., Olson, J. E., Eichhubl, P., and Fall, A. (2014). Natural fractures in shale: a review and new observations. *AAPG Bull.* 98 (11), 2165–2216. doi:10.1306/08121413151

Gong, X. X., Shi, Z. J., Wang, Y., Tian, Y. M., Li, W. J., and Liu, L. (2017). Characteristics and origin of the relatively high-quality tight reservoir in the Silurian Xiaoheba Formation in the southeastern Sichuan Basin. *PLOS One* 12 (7), e0180980. doi:10.1371/journal.pone.0180980

Guo, T. L., Xiong, L., Lei, W., Zhao, Y., and Pang, H. Q. (2022). Deep shale gas exploration and development in the Weirong and Yongchuan areas, South Sichuan Basin: progress, challenges and prospect. *Nat. Gas. Ind.* 42 (8), 45–59. doi:10.3787/j.issn.1000-0976.2022.08.005

Guo, X. S., Li, Y. P., Liu, R. B., and Wang, Q. B. (2014). Characteristics and controlling factors of micro-pore structures of Longmaxi shale play in the jiaoshiba area, Sichuan Basin. *Nat. Gas. Ind.* 34 (6), 9–16. doi:10.3787/j.issn.1000-0976.2014.06.002

Hakimi, M. H., Hamed, T. E., Lotfy, N. M., Radwan, A. E., Lashin, A., and Rahim, A. (2023). Hydraulic fracturing as unconventional production potential for the organic-rich carbonate reservoir rocks in the Abu El Gharadig Field, north western Desert (Egypt): evidence from combined organic geochemical, petrophysical and bulk kinetics modeling results. *Fuel* 334 (1), 126606. doi:10.1016/j.fuel.2022.126606

Hatch, J. R., and Leventhal, J. S. (1992). Relationship between inferred redox potential of the depositional environment and geochemistry of the upper pennsylvanian (missourian) Stark shale member of the dennis limestone, wabaunsee county, Kansas, USA. *Chem. Geol.* 99, 65–82. doi:10.1016/0009-2541(92)90031-Y

He, S., Li, H., Qin, Q. R., and Long, S. X. (2021). Influence of mineral compositions on shale pore development of Longmaxi Formation in the Dingshan area, southeastern Sichuan Basin, China. *Energy Fuel* 35 (13), 10551–10561. doi:10.1021/acs.energyfuels.1c01026

He, S., Qin, Q. R., Li, H., and Zhao, S. X. (2022). Deformation differences in complex structural areas in the southern sichuan Basin and its influence on shale gas preservation: a case study of changning and luzhou areas. *Front. Earth Sci.* 9, 818543. doi:10.3389/feart.2021.818534

He, S., Tan, W. C., Li, H., Wang, Y., Niu, P. F., and Qin, Q. R. (2025). Mineralogical and lithofacies controls on gas storage mechanisms in organic-rich marine shales. *Energy Fuel* 39 (7), 3846–3858. doi:10.1021/acs.energyfuels.4c05685

He, W., Li, T., Mou, B. X., Lei, Y. X., Song, J. H., and Liu, Z. C. (2023). Lithofacies types and physical characteristics of organic-rich shale in the Wufeng-Longmaxi Formation, Xichang Basin, China. *ACS Omega* 8 (20), 18165–18179. doi:10.1021/acsomega.3c01307

Hou, H. D., Yang, W., Yang, R., Jiang, Z. X., Miao, K., Sun, W. H., et al. (2025). Formation and evolution of complex pore-fracture systems in shale gas reservoirs: insights into controlling mechanisms. *Energy Fuel* 39 (6), 3008–3038. doi:10.1021/acs.energyfuels.4c05306

Houseknecht, D. W. (1987). Assessing the relative importance of compaction processes and cementation reduction of porosity in sandstone. *AAPG Bull.* 71 (5), 485–491. doi:10.1306/9488787F-1704-11D7-8645000102C1865D

Hu, H. Y., Wang, D. X., Li, W. P., Zhu, G. E., and Chen, X. Y. (2025). The heterogeneity characterization of lacustrine shale pores in the daanzhai member of the ziliujing Formation in the yuanba area, Sichuan Basin. *Minerals* 15 (1), 11. doi:10.3390/min15010011

Iacoviello, F., Lu, X. K., Mitchell, T. M., Brett, D. J. L., and Shearing, P. R. (2019). The imaging resolution and knudsen effect on the Mass transport of shale gas assisted by multi-length scale X-ray computed tomography. *Sci. Rep.* 9, 19465. doi:10.1038/s41598-019-55999-7

Jadoon, Q. K., Roberts, E., Blenkinsop, T., Wust, R. A. J., and Shah, S. A. (2016). Mineralogical modelling and petrophysical parameters in Permian gas shales from the Roseneath and Murteree formations, Cooper Basin, Australia. *Petrol. explor. Dev.* 43 (2), 277–284. doi:10.1016/S1876-3804(16)30031-3

Jiang, S. L., Tang, T., Zhong, S. C., Li, H., Gao, Z., Yang, C., et al. (2023). Intensive geological alteration and gas accumulation in Longmaxi Formation shales at moderate and great depths: a case study of the Luzhou area in the southern Sichuan fold zone, China. *Geol. J.* 8 (48), 4215–4228. doi:10.1002/gj.4788

Jin, Z. J., Liang, X. P., and Bai, Z. R. (2022). Exploration breakthrough and its significance of Gulong lacustrine shale oil in the Songliao Basin, Northeastern China. *Energy Geosci.* 3 (2), 120–125. doi:10.1016/j.engeos.2022.01.005

Jones, B. J., and Manning, A. C. (1994). Comparison of geochemical indices used for the interpretation of palaeoredox conditions in ancient mudstones. *Chem. Geol.* 111 (1-4), 111–129. doi:10.1016/0009-2541(94)90085-X

Jun, J., and Liang, W. (2024). Investigation of the pore structure characteristics and fluid components of Quaternary mudstone biogas reservoirs: a case study of the Qaidam Basin in China. *Sci. Rep.* 14 (1), 26512. doi:10.1038/s41598-024-78010-4

Kasala, E. E., Wang, J. J., Majid, A., and Nadege, M. N. (2025). Enhancing CO2 storage capacity and methane (CH4) production in the Yanchang shale gas reservoir: a simulation study on influencing factors and optimization strategies. *Fuel* 388, 134535. doi:10.1016/j.fuel.2025.134535

Li, H. (2022). Research progress on evaluation methods and factors influencing shale brittleness: a review. *Energy Rep.* 8, 4344–4358. doi:10.1016/j.egyr.2022.03.120

Li, H. (2023a). Advancing "carbon peak" and "carbon neutrality" in China: a comprehensive review of current global research on carbon capture, utilization, and storage technology and its implications. *ACS Omega* 8 (45), 42086–42101. doi:10.1021/acsomega.3c06422

Li H, H., Duan, H. T., Qin, Q. R., Zhao, T. B., Fan, C. H., and Luo, J. (2025). Characteristics and distribution of tectonic fracture networks in low permeability conglomerate reservoirs. *Sci. Rep.* 15 (1), 5914. doi:10.1038/s41598-025-90458-6

Li, H., He, S., Radwan, A. E., Xie, J. T., and Qin, Q. R. (2024a). Quantitative analysis of pore complexity in lacustrine organic-rich shale and comparison to marine shale: insights from experimental tests and fractal theory. *Energy Fuel* 38 (17), 16171–16188. doi:10.1021/acs.energyfuels.4c03095

Li, H., Tang, H. M., Qin, Q. R., Zhou, J. L., Qin, Z. J., Fan, C. H., et al. (2019). Characteristics, formation periods and genetic mechanisms of tectonic fractures in the

tight gas sandstones reservoir: a case study of Xujiahe Formation in YB area, Sichuan Basin, China. *J. Petrol. Sci. Eng.* 178, 723–735. doi:10.1016/j.petrol.2019.04.007

Li, H., Wang, Q., Qin, Q. R., and Ge, X. Y. (2021). Characteristics of natural fractures in an ultradeep marine Carbonate gas reservoir and their impact on the reservoir: a case study of the Maokou Formation of the JLS Structure in the Sichuan Basin, China. *Energy Fuel* 35 (16), 13098–13108. doi:10.1021/acs.energyfuels.1c01581

Li H, H., Zhou, J. L., Mou, X. Y., Guo, H. X., Wang, X. X., An, H. Y., et al. (2022). Pore structure and fractal characteristics of the marine shale of the Longmaxi Formation in the changning area, southern Sichuan Basin, China. *Front. Earth Sci.* 10, 1018274. doi:10.3389/feart.2022.1018274

Li, J., Li, H., Jiang, W., Cai, M. L., He, J., Wang, Q., et al. (2024b). Shale pore characteristics and their impact on the gas-bearing properties of the Longmaxi Formation in the Luzhou area. *Sci. Rep.* 14, 16896. doi:10.1038/s41598-024-66759-7

Li J, J., Li, H., Xu, J. L., Wu, Y. J., and Gao, Z. (2022). Effects of fracture formation stage on shale gas preservation conditions and enrichment in complex structural areas in the southern Sichuan Basin, China. *Front. Earth Sci.* 10, 921988. doi:10.3389/feart.2022.921988

Li, J. J., You, H., Zhang, X. W., Zhao, S. P., Jiang, F. J., Feng, G. Q., et al. (2024c). Influence of shale reservoir properties on shale oil mobility and its mechanism. *Energy Geosci.* 5 (4), 100329. doi:10.1016/j.engeos.2024.100329

Li, Q. W., Liu, Z. B., Chen, F. R., Zhang, K., and Tang, L. (2023). Behavior and controlling factors of methane adsorption in Jurassic continental shale, northeastern Sichuan Basin. *Energy Geosci.* 4 (1), 83–92. doi:10.1016/j.engeos.2022.08.007

Liu G. Y, G. Y., Tang, Y., Liu, K. Q., Liu, Z. Q., Zhu, T., Zou, Y., et al. (2024). Comparison of pore structure characteristics of shale-oil and tight-oil reservoirs in the Fengcheng Formation in Mahu Sag. *Energies* 17 (16), 4027. doi:10.3390/en17164027

Liu J, J., He, X., and Xue, F. (2024). The influence of natural fractures of multi-feature combination on seepage behavior in shale reservoirs. *J. Min. Strata Control Eng.* 6 (1), 013437. doi:10.13532/j.jmsce.cn10-1638/td.20240018.001

Luo, J. L., Guo, D. Y., Yi, P., Wang, Z. Z., and Yang, J. L. (2003). Major factors controlling reservoir-quality of the Upper Triassic Chang 2 sandstones in the Panlong oil area. *J. Northwest Univ.* 33 (6), 105–110. doi:10.16152/j.cnki.xdxbzr.2003.06.035

Ma, Y., and Feng, J. L. (2023). Depositional environment variations and organic matter accumulation of the first member of the Qingshankou Formation in the southern Songliao Basin, China. *Front. Earth Sci.* 11, 1249787. doi:10.3389/feart.2023.1249787

Milkov, A. V., Schwietzke, S., Allen, G., Sherwood, O. A., and Etiope, G. (2020). Using global isotopic data to constrain the role of shale gas production in recent increases in atmospheric methane. *Sci. Rep.* 10, 4199. doi:10.1038/s41598-020-61035-w

Nag, R., Cogne, N., Hrushikesh, H., Prabhakar, N., and Mishra, D. (2025). Petrochronology and geochemistry of migmatites from the Assam-Meghalaya gneissic complex (NE India): implications for the crustal anatexis and reworking during Gondwana assembly. *Precambrian Res.* 418, 107670. doi:10.1016/j.precamres.2024.107670

Peng, J., Zhang, H. B., and Lin, X. X. (2018). Study on characteristics and genesis of botryoidal dolostone of the Upper Sinian Dengying Formation: a case study from Hanyuan region, Sichuan, China. *Evaporite* 33 (2), 285–299. doi:10.1007/s13146-017-0343-8

Peng, M. H., Li, J., Tian, J. C., Zhang, X., Luo, J., Li, P. J., et al. (2025). Neoproterozoic rifting along the margin of the rodinia supercontinent: sedimentary evidence from the northwestern tarim block, northwest China. *Palaeogeogr. Palaeocl.* 660, 112662. doi:10.1016/j.palaeo.2024.112662

Qin, L. M., and Lan, X. D. (2024). Genesis of the wuchiapingian formation tuffs and their relationship with the tectonic background of the kaijiang-liangping trough in the northern Sichuan Basin. *Minerals* 14 (10), 1034. doi:10.3390/min14101034

Qiu, H. Y., Jiang, Z. X., Liu, Z. J., Chang, J. Q., Su, Z. F., Yang, Z. W., et al. (2021). Difference in pore structure characteristics between condensate and dry shale gas reservoirs: insights from the pore contribution of different matrix components. *J. Nat. Gas. Sci. Eng.* 96, 104283. doi:10.1016/j.jngse.2021.104283

Radwan, A. E., Wood, D. A., and Radwan, A. A. (2022). Machine learning and data-driven prediction of pore pressure from geophysical logs: a case study for the Mangahewa gas field, New Zealand. *J. Rock Mech. Geotech.* 14 (6), 1799–1809. doi:10.1016/j.jrmge.2022.01.012

Radwan, A. E., Yin, S., Hakimi, M. H., and Li, H. (2023). Petroleum geology of conventional and unconventional resources: introduction. *Geol. J. (Chichester).* 58 (11), 3965–3969. doi:10.1002/gj.4898

Sohail, G. M., Radwan, A. E., and Mahmoud, M. (2022). A review of Pakistani shales for shale gas exploration and comparison to North American shale plays. *Energy Rep.* 8, 6423–6442. doi:10.1016/j.egyr.2022.04.074

Sun, Z. M. (2023). Superimposed hydrocarbon accumulation through multi-source and multi-stage evolution in the Cambrian Xixiangchi Group of eastern Sichuan Basin: a case study of the Pingqiao gas-bearing anticline. *Energy Geosci.* 4 (1), 131–142. doi:10.1016/j.engeos.2022.09.001

Tan, J., Jiang, Y. Q., Li, X. T., Ji, C. H., Gu, Y. F., and Wang, Z. L. (2024). Paleoenvironment of marine-continental transitional shales in the lower Permian Shanxi formation, southeastern Ordos Basin, China. *Energy Geosci.* 5 (3), 100261. doi:10.1016/j.engeos.2023.100261

Tang, S. Q., Dong, S. F., Yang, X. Y., Fan, C. H., Li, H., Zhong, Z. Y., et al. (2023). Geochemical analysis of dolomite in the fourth member of the upper sinian dengying formation, northern Sichuan Basin, China. *ACS Omega* 8 (48), 45878–45895. doi:10.1021/acsomega.3c06638

Wan, J. L., Yu, Z. C., Yuan, Y. J., Huang, W. H., Dong, Z. T., and Rezaee, R. (2025). Lithofacies classification and reservoir property of lacustrine shale, the Cretaceous Qingshankou formation, Songliao basin, northeast China. *Mar. Petrol. Geol.* 173, 107262. doi:10.1016/j.marpetgeo.2024.107262

Wang B, B., Lu, C. L., Cui, F., and Zhang, Z. (2023). Uniaxial compression test research on rock creep disturbance characteristics based on CT scanning. *J. Min. Strata Control Eng.* 5 (3), 43–53. doi:10.13532/j.jmsce.cn10-1638/td.2023.03.002

Wang E. Z, E. Z., Guo, T. L., Li, M. W., Xiong, L., Dong, X. X., Wang, T., et al. (2023). Favorable exploration lithofacies and their formation mechanisms in lacustrine shales deposited under different salinity conditions: insights into organic matter accumulation and pore systems. *Energy Fuel* 37 (16), 11838–11852. doi:10.1021/acs.energyfuels.3c02038

Wang, J., and Wang, X. L. (2021). Seepage characteristic and fracture development of protected seam caused by mining protecting strata. *J. Min. Strata Control Eng.* 3 (3), 58–66. doi:10.13532/j.jmsce.cn10-1638/td.20201215.001

Wang, R. F., and Tang, Y. (2023). Study on the rock physical mechanical properties evaluation of tight oil reservoir in Chang 7 member, Longdong area, Ordos Basin, China. *Front. Earth Sci.* 11, 1249787. doi:10.3389/feart.2024.1342561

Wen, Z., Yao, Y. B., Sun, X. X., Lei, X., and Cui, C. (2024). The impact of gas flow on hydrate reformation and reservoir seepage characteristics in clayey silt sediments. *Energy Fuel* 38 (6), 5149–5158. doi:10.1021/acs.energyfuels.3c05096

Wu, H. J., and Kong, X. W. (2025). Analysis of geological characteristics and potential factors of formation damage in coalbed methane reservoir in Northern Qinshui basin. *Sci. Rep.* 15 (1), 3025. doi:10.1038/s41598-025-87026-3

Wu, X. Q., Yang, J., Wang, P., Li, H. J., Chen, Y. B., Ni, C. H., et al. (2024). Gas source of the middle jurassic Shaximiao Formation in the zhongjiang large gas field of western sichuan depression: constraints from geochemical characteristics of light hydrocarbons. *Energy Geosci.* 5 (2), 100263. doi:10.1016/j.engeos.2023.100263

Yang L. R, L. R., Li, J. J., and Jiang, C. (2022). Analysis of acoustic emission parameters and time-frequency characteristics in the process of rock sample fracture. *J. Min. Strata Control Eng.* 5 (1), 013015. doi:10.13532/j.jmsce.cn10-1638/td.20220923.003

Yang, S. P., Liu, P. Z., and Lu, W. Y. (2023). Study on triaxial compression tests on briquette coal specimens with different binder contents. *J. Min. Strata Control Eng.* 5 (2), 023027. doi:10.13532/j.jmsce.cn10-1638/td.2023.02.001

Yang Y. M, Y. M., Peng, J., Xu, T. Y., Wang, Y. B., and Zeng, Y. (2022). Characterization, classification, and evaluation of the reservoir pore structure features of lacustrine fine-grained sedimentary rocks. A case study of the fourth member of the shahejie Formation in the chenguanzhuang area of the southern gently sloping zone of the dongying depression, bohai bay basin. *Front. Earth Sci.* 10, 878089. doi:10.3389/feart.2022.878089

Ye, T. R., Meng, J., Xiao, Y. T., Liu, y.q., Zheng, A. W., and Liang, B. (2025). Integrated AutoML-based framework for optimizing shale gas production: a case study of the Fuling shale gas field. *Energy Geosci.* 6 (1), 100365. doi:10.1016/j.engeos.2024.100365

Yuan, D. D., Lu, S. F., Chen, F. W., Xiao, H., and Wu, Y. H. (2016). Shale microscopic pore structure characterization in well Pengye 1 of southeast Chongqing. *Spec. Oil Gas. Res.* 23 (1), 49–53. doi:10.3969/j.issn.1006-6535.2016.01.011

Zhang, B. L., Shen, B. T., Zhang, J. H., and Zhang, X. G. (2020). Experimental study of edge-opened cracks propagation in rock-like materials. *J. Min. Strata Control Eng.* 2 (3), 033035. doi:10.13532/j.jmsce.cn10-1638/td.20200313.001

Zhang, J. G., Jiang, Z. X., Liu, L., Yuan, F., Feng, L. Y., and Li, C. S. (2021). Lithofacies and depositional evolution of fine-grained sedimentary rocks in the lower submember of the Member 3 of Shahejie Formation in Zhanhua sag, Bohai Bay Basin. *Acta petro. Sin.* 42 (3), 293–306. doi:10.7623/syxb202103003

Zhang, S., Liu, H. M., Wang, M., Fu, A. B., Bao, S. Y., Wang, W. Q., et al. (2018). Pore evolution of shale oil reservoirs in Dongying sag. *Acta Petrol. Sin.* 39 (7), 754–766. doi:10.7623/syxb201807003

Zhao, D. F., Jiao, W. W., and Wei, Y. (2021). Diagenesis of a shale reservoir and its influence on reservoir brittleness: taking the deep shale of the Wufeng-Longmaxi Formation in western chongqing as an example. Acta sediment. *Sin.* 39 (4), 811–825. doi:10.14027/j.issn.1000-0550.2021.034

Zhao, J. H., and Jin, Z. J. (2021). Mudstone diagenesis: research advances and prospects. *Acta Sediment. Sin.* 39 (1), 58–72. doi:10.14027/j.issn.1000-0550.2020.133

Zhou, Q. M., Xu, H., Zhou, W., Zhao, X., Liu, R. Y., and Jiang, K. (2025). Sealing effects on organic pore development in marine shale gas: new insights from macro-to micro-scale analyses. *Energies* 18 (1), 193. doi:10.3390/en18010193